Published online 20 September 2018 *Nucleic Acids Research, 2018, Vol. 46, No. 19* ***10225–10245***
doi: 10.1093/nar/gky841

COPII vesicles can affect the activity of antisense oligonucleotides by facilitating the release of oligonucleotides from endocytic pathways

Xue-hai Liang*, Hong Sun, Joshua G. Nichols, Nickolas Allen, Shiyu Wang, Timothy A. Vickers, Wen Shen, Chih-Wei Hsu and Stanley T. Crooke

Core Antisense Research, Ionis Pharmaceuticals, Inc. 2855 Gazelle Court, Carlsbad, CA 92010, USA

Received June 29, 2018; Revised August 23, 2018; Editorial Decision September 07, 2018; Accepted September 10, 2018

ABSTRACT

RNase H1-dependent, phosphorothioate-modified antisense oligonucleotides (PS-ASOs) can enter cells through endocytic pathways and need to be released from the membrane-enclosed organelles, a limiting step for antisense activity. Accumulating evidence has suggested that productive PS-ASO release mainly occurs from late endosomes (LEs). However, how PS-ASOs escape from LEs is not well understood. Here, we report that upon PS-ASO incubation, COPII vesicles, normally involved in ER–Golgi transport, can re-locate to PS-ASO-containing LEs. Reduction of COPII coat proteins significantly decreased PS-ASO activity, without affecting the levels of PS-ASO uptake and early-to-late endosome transport, but caused slower PS-ASO release from LEs. COPII co-localization with PS-ASOs at LEs does not require *de novo* assembly of COPII at ER. Interestingly, reduction of STX5 and P115, proteins involved in tethering and fusion of COPII vesicles with Golgi membranes, impaired COPII re-localization to LEs and decreased PS-ASO activity. STX5 can re-locate to LEs upon PS-ASO incubation, can bind PS-ASOs, and the binding appears to be required for this pathway. Our study reveals a novel release pathway in which PS-ASO incubation causes LE re-localization of STX5, which mediates the recruitment of COPII vesicles to LEs to facilitate endosomal PS-ASO release, and identifies another key PS-ASO binding protein.

INTRODUCTION

Antisense oligonucleotides (ASOs) have been developed and used as both research tools and therapeutic agents by modulating gene expression via different mechanisms, and several ASO drugs have been approved by FDA and multiple drugs are on clinical trials to treat various diseases (1–5). RNase H1-dependent ASOs are designed as gapmer configuration, with ∼10 deoxynucleotides in the center to support RNase H1 activity to degrade target RNAs, and the flanking sequences (3–5 nts at each end) contain 2′-modified nucleotides to enhance drug performance (6). Commonly used 2′ modifications include but not limited to 2′-*O*-methyloxylethyl (MOE), constrained ethyl or locked nucleic acids (LNA). In addition, ASOs are linked with phosphorothioate (PS) backbone, which has been shown to ensure efficient ASO delivery and cellular uptake, in addition to other pharmacological benefits (7–9).

PS-ASOs exhibit stronger binding affinity to proteins relative to phosphodiester (PO) backbone ASOs, and ASO–protein interactions can affect ASO performance, which is also influenced by other factors, such as RNA structure, splicing and translation (3,10–16). The tighter protein binding property can prevent PS-ASOs from being excreted and ensure sufficient ASOs reach target tissues to achieve pharmacological activities (17,18). PS-ASOs can interact with cell surface proteins, e.g. stablin, asialoglycoprotein receptor (ASGR) and Epidermal growth factor receptor (EGFR), which can mediate ASO uptake mainly through endocytic pathways (19–21), although ASOs can also enter cells via macropinocytosis especially at high ASO concentrations (9,22–24). After internalization, however, only a small portion of cellular ASOs appear to be active, as the majority of ASOs remain entrapped in membrane-enclosed organelles (25). Thus, ASO release from endocytic pathways is a major limiting factor for ASO delivery to target RNAs (9,26,27).

Internalized ASOs can traffic through early endosomes (EE) within 10–30 min, transport to late endosomes (LEs) within 20–60 min and ultimately reach the lysosomes (9,28). Previous studies suggested that ASOs present in lysosomes are not active, and ASO release that leads to antisense activity (productive release) most likely occurs from LEs, and not from EEs (9,25,28–31). We recently found that upon ASO incubation, Annexin A2 (ANXA2), a lipid binding

*To whom correspondence should be addressed. Tel: +760 603 3816; Fax: +760 603 2600; Email: lliang@ionisph.com

© The Author(s) 2018. Published by Oxford University Press on behalf of Nucleic Acids Research.
This is an Open Access article distributed under the terms of the Creative Commons Attribution Non-Commercial License (http://creativecommons.org/licenses/by-nc/4.0/), which permits non-commercial re-use, distribution, and reproduction in any medium, provided the original work is properly cited. For commercial re-use, please contact journals.permissions@oup.com

protein that localizes to EE and is required for EE to LE transport (32), re-located to LE and was present on LEs and at intraluminal vesicles (ILVs) inside LEs, or multivesicular bodies (MVBs) (28). Reduction of ANXA2 delayed ASO trafficking from EE to LE and reduced ASO activity. Kinetic studies suggested that productive ASO release mainly occurs from LEs, and can be mediated by a back-fusion process involving the fusion of ILV membrane and LE limiting membrane, leading to the release of ILV contents (9,28,30). Further, we demonstrated that lysobisphosphatidic acid (LBPA), a late endosome/ILV specific lipid, is involved in ASO release from LEs and can affect ASO activity (30). LBPA is required for LE membrane deformation and for ILV formation (33). Inactivation of LBPA using an antibody or reduction of the LBPA level by small interfering RNA (siRNA)-mediated reduction of ALIX (ALG-2 interacting protein X) decreased ASO activity and localization in ILVs, without affecting ASO uptake (30). These results further suggest that ASO release from LE via a back-fusion process contributes to ASO activity. However, as not all LE-localized ASOs are present in ILVs, and inhibition of LBPA only partially reduced ASO activity, it is possible that multiple pathways of ASO release from LEs may exist that act together to contribute to ASO activity (9). Nevertheless, information on the pathways of ASO release from LEs is still very limited. Identifying new pathways and understanding the detailed mechanisms of transport and release are thus important for enhancing ASO release and therefore drug potency.

Inside cells, multiple membraned vesicles exist that are involved in different intracellular transport pathways of biological materials. One such vesicle is coat protein complex II (COPII), which is required for anterograde transport of many newly synthesized proteins from endoplasmic reticulum (ER) to Golgi, including membrane proteins and secreted proteins (34–36). COPII vesicles are assembled in a stepwise process on ER membranes, specifically the ER exit site (ERES), where cargo proteins emerge (37–39). Initiation of COPII assembly requires the activation of the small GTPase Sar1 by SEC12, an ER-bound transmembrane guanine nucleotide exchange factor for Sar1 (40). COPII assembly may also require SEC16, another ERES localized protein (41,42). Subsequently, pre-assembled SEC23/SEC24 sub-complex interacts with Sar1, forming a pre-budding complex. Next, SEC13/SEC31 sub-complex joins and forms the outer layer coat. These five proteins (Sar1, SEC23/SEC24, SEC13/SEC31) constitute the minimum coat proteins of COPII vesicles, as determined in *in vitro* reconstitution studies (38,43–45). After membrane deformation, the cargo-containing COPII vesicles bud from ER, traffic via the microtubule network, and reach the ER–Golgi intermediate complex (ERGIC), where the cargo continues to move forward to Golgi and ultimately to its destination (36,46). The tethering and fusion of COPII vesicles with Golgi membranes require additional proteins, such as the docking protein P115 and the SNARE protein STX5 (47–51). The membrane materials return to the ER through the retrograde transport pathway via coat protein complex I (COPI) vesicles, which contain ARF1, another small GTPase and other coat proteins such as coatomer subunit beta (β-COP) (38).

To better understand how ASOs are released from membrane-enclosed organelles and traffic inside cells, we have been characterizing the effects of different transport pathways on ASO activity and distribution. Here, we report that upon ASO incubation, COPII vesicles can co-localize with ASOs mainly at LEs. Such ASO/COPII co-localization does not require *de novo* COPII assembly on ERES, suggesting that budded COPII vesicles are recruited to LEs upon ASO incubation. COPII/ASO co-localization at LEs is affected by STX5 and P150, proteins involved in normal COPII vesicle interactions with Golgi membranes. STX5 binds to PS-ASOs and it can re-locate to LE upon ASO incubation, likely mediated by ASO–protein interactions. Importantly, reduction of COPII proteins, as well as STX5 and P115, significantly reduced ASO activity. Kinetic studies suggest that reduction of COPII proteins did not affect ASO uptake and transport from EE to LEs, rather, ASO release was decreased. Together, our results indicate that COPII vesicles can be recruited to LEs in a STX5-dependent manner, and can enhance ASO activity by facilitating ASO release from LEs.

MATERIALS AND METHODS

ASOs, siRNAs, antibodies and primer probe sets for qRT-polymerase chain reaction (PCR) are listed in Supplementary Data.

Cell culture and transfection

HeLa, A431, HepG2 or SVGA astrocyte cells expressing GFP-Rab7 (a kind gift from Dr Tomas Kirchhausen's lab) were cultured in Dulbecco's modified Eagle's medium supplemented with 10% fetal bovine serum (FBS), 0.1 μg/ml streptomycin and 100 units/ml penicillin. Normal human primary neonatal dermal fibroblast (HDFn) cells (Life Technologies) were grown in 106 medium supplemented with low serum growth supplements (Life Technologies). Cells were seeded at ∼60% confluency and grown for 16 h before transfection. siRNA was transfected into cells using Lipofectamine RNAiMax (Life Technologies), at 3–6 nM final siRNA concentration. For ASO activity assays under free uptake, HeLa or A431cells were treated or not treated with siRNAs for 48 h, or as indicated in figure legends. Cells were then re-seeded in 96-well plates at ∼75% confluency. After 8 h, ASOs were added to the medium and cells were continued to grow for overnight before RNA preparation. For ASO transfection, siRNA-treated cells were re-seeded in 96-well plates, incubated for overnight, and ASOs were transfected for 4 h using Lipofectamine 2000 (Life Technologies).

RNA preparation and qRT-PCR analysis

RNA preparation and qRT-PCR assay using TaqMan primer probe sets were performed as described previously (16). Briefly, total RNA was prepared using RNeasy mini kit (Qiagen). qRT-PCR was performed in triplicate using StepOne Real-Time PCR system and TaqMan primer probe sets with Ag-PathID™ One-step RT-PCR kit (Applied Biosystems). qRT-PCR in 20 μl reactions was performed using the following program: 48°C for 10 min, 94°C

for 10 min and 40 cycles of 20 s each at 94°C and 60°C. The qRT-PCR results were quantified using StepOne Software V2.3, calculated and plotted using Excel. Target RNA levels were normalized to the levels of total RNA measured using SYBR Green (Life Technologies). Statistics analysis was performed using Prism, with *F*-test for curve comparison based on non-linear regression (dose–response curves) for XY analyses, using equation 'log(agonist) versus normalized response –Variable slop'. The *Y* axis (relative messenger RNA (mRNA) level) was directly used as the normalized response.

Western analysis

Cells were collected using trypsin, or using scraper in 1× phosphate buffered saline (PBS) buffer when detecting cell surface proteins, and washed once with 1× PBS. Cell lysate was prepared using radioimmunoprecipitation assay (RIPA) buffer (ThermoFisher) and cleared by centrifugation at 10 000 × g for 10 min at 4°C. Proteins (20–40 μg/lane) were separated by 4–12% sodium dodecyl sulphate-polyacrylamide gel electrophoresis (SDS-PAGE), transferred to membranes using iBlot transfer system (Life Technologies), and proteins were detected with specific antibodies, and visualized using enhanced chemiluminescence (ECL), as described previously (13).

Immunofluorescent staining

Cells were washed with 1× PBS, fixed with 4% paraformaldehyde for 0.5–1 h at room temperature and permeabilized for 4 min with 0.1% Triton in 1× PBS. After blocking at room temperature for 30 min with block buffer (1 mg/ml bovine serum albumin in 1× PBS), cells were incubated with primary antibodies (1:100–1:300) in block buffer for 2–4 h, washed three times (5 min each) using wash buffer [0.1% nonyl phenoxypolyethoxylethanol-40 (NP-40) in 1× PBS] and incubated for 1 h with secondary antibody conjugated with fluorophores (1:200). After washing three times, cells were mounted with Anti-fade reagent containing DAPI (Life Technologies), and images were acquired using confocal microscope (Olympus FV-1000) and processed using FV-10 ASW 3.0 Viewer software (Olympus). Z-stacks were generated from images taken at 0.1–0.11 μm depth per section, and 3D images or movies were generated using FV-10 ASW-3.0 viewer. For early time staining after ASO incubation (within 2 h), cells were washed three times with acidic buffer (0.1 M acetic acid, 500 mM NaCl) and one time with 1× PBS, to remove cell surface-associated ASOs before fixation. Quantification of co-localization events was performed manually from ∼20 cells, by counting overlapping foci of which images from both channel have clearly defined boundary without saturation. Statistics analysis was performed based on unpaired *t*-test using prism.

Affinity selection

Affinity selection using biotinylated ASO IONIS386652 was performed as described previously (52). Proteins were eluted using PS-MOE gapmer ASO IONIS116847, or a 2′-*O*-methylated PO-ASO XL273.

BRET assay for ASO-binding affinity to proteins

Amino-terminal NLuc fusions were created using the vector pFN31K Nluc CMV-neo (Promega). Briefly, Sar1a and SEC13 were amplified from the plasmids RC201450 and SC111014 (Origene) using PCR. The forward PCR primer was comprised of sequence following the AUG start codon preceded by a XhoI site, whereas the reverse primer was complementary to the sequence preceding the stop codon followed by an EcoRI site. Sar1a primers: N-F, 5′-gcattcgaCTCGAGCTCTTTCATCTTTG AGTGGATCTAC; N-R, 5′- CTGGCTCTCCCAGTAT ATTGACtaggaattcgcattcga. SEC13 primers: N-F, 5′-gcattcgaCTCGAGCGTGTCAGTAATTAACACTGTGG AT; N-R 5′-GCCAGCAGAACGAGCAGTGAtaggaattcg cattcga. The PCR product was digested with XhoI and EcoRI then ligated into the pFN31K Nluc CMV-neo vector. A 6× HIS-tag (CAT CATCATCACCACCAC) was inserted upstream of the NLuc cassette by site directed mutagenesis using a Q5 Site-Directed Mutagenesis Kit (New England BioLabs). STX5 (NM_003164) was amplified by PCR from the full-length complementary DNA clone (Origene SC118144). The forward PCR primer (5′ gctagcAGCCACC**ATG**ATCC CGCGGAAACGCTA -3′) was comprised of sequence complimentary to the STX5 sequence, including the **ATG** start codon and preceded by a Kozak sequence and an NheI site (GC-TAGCAGCCACC), whereas the reverse primer (5′-CATCTTTGTGGTCTTCCT TGCgactcgag) was complementary to the STX5 sequence up to amino acid 355, then followed with an XhoI site. The PCR product was ligated into NheI and XhoI sites of the NanoLuc expression vector pFC32K Nluc CMV-Neo (Promega) with a 6× HIS-tag (CATCATCATCACCACCAC) inserted downstream of the NLuc cassette by site-directed mutagenesis using a Q5 Site-Directed Mutagenesis Kit (New England BioLabs) according to the manufacturer's protocol.

Fusion proteins were expressed by transfecting the plasmids into 6 × 10^5 HEK 293 cells using Effectene (Qiagen). Following a 24-h incubation, cells were collected by trypsinization, washed with 1× PBS, then resuspended in 250 μl Pierce IP Lysis Buffer (Thermo Scientific). Lysates were incubated 30 min at 4°C while rotating, then debris pelleted by centrifugation at 15 000 rpm for 5 min. The fusion protein was purified by adding 20 μl HisPur Ni-NTA Magnetic Beads (Thermo Scientific) and 10 mM imidazole then incubating at 4°C for 2 h. Beads were then washed four times with 1× PBS + 10 mM imidazole and 0.01% Tween-20. Fusion protein was eluted from the beads in 100 μl 1× PBS + 200 mM imidazole, followed by dilution with 200 μl IP buffer.

Bioluminescence resonance energy transfer (BRET) binding affinity assays were performed as described (53). Alexa-linked ASOs (766634) at the indicated concentrations were incubated at room temperature for 15 min in 1× binding buffer with 10^6 RLU/well of Ni-NTA purified NLuc fusion protein or whole cell lysate. Following the incubation, NanoGlo substrate (Promega) was added at 0.1 μl/well. Readings were performed for 0.3 s using a Glomax Discover system using 450 nm/8 nm bandpass for the donor filter, and 600 nm long pass for the acceptor filter. BRET was cal-

culated as the ratio of the emission at 600/450 nm [fluorescent excitation emission/relative light units (RLU)]. For competitive binding assays, the Alexa-linked ASO (766635) was added at approximately the k_d, and the unconjugated competing ASOs (XL948-XL952) added at the indicated concentrations in 50 μl water. About 10^6 RLU/well of purified fusion protein or whole cell lysate well was then added in 50 μl 2× binding buffer for a final volume of 100 μl. After incubation at room temperature for 15 min, substrate addition and BRET readings were carried out as detailed above.

Glycoprotein protein staining

HeLa cells grown in 10 cm dishes with serum-free medium (Life Technologies) were incubated with or without 10 μM ASO116847 for 24 h, and 1 ml medium was collected and cleared by centrifugation at 2000 × g for 4 min. Proteins in the medium were precipitated using trichloroacetic acid . Cells were collected using scrapper, washed and cellular proteins were prepared using RIPA buffer. The precipitated proteins from the medium and 30 μg cellular protein were separated on a 4–12% SDS-PAGE gel. The gel was stained for glycoprotein using Glycoprotein Detection Kit (Sigma). Subsequently, the gel was stained again using Coomassie blue to visualize total proteins.

ASO uptake assay

HeLa cells treated with different siRNAs for 48 h were reseeded in 96 plates, incubated for overnight and Cy3-labeled PS-ASO (IONIS446654) was added to the medium. After 3 h, cells were washed with 1× PBS, trypsinized and resuspended in 1× PBS supplemented with 3% FBS for analysis by flow cytometry using an Attune NxT Flow Cytometer (ThermoFisher Scientific).

RESULTS

COPII vesicles can co-localize with ASOs

To better understand the mechanisms of ASO endocytic release and intracellular trafficking, we sought to determine whether ASOs can co-localize with cellular vesicles other than endosomal organelles. The active and dynamic trafficking vesicles in the ER–Golgi transport pathways, including the COPII vesicles mediating anterograde transport and COPI vesicles mediating the retrograde transport between ER and Golgi, appear to be attractive candidates. For this purpose, we stained a COPII coat protein, SEC31a, in HeLa cells incubated for 16 h with a Cy3-labeled PS/MOE gapmer ASO (IONIS446654) by free uptake, i.e. without transfection reagents. We note that PS-backbone ASOs were used throughout the study, unless specified. In addition, we recommend visualizing the confocal images on screen for better resolution. Consistent with previous observations (52), ASOs delivered by free uptake were typically localized as punctate structures in the cytoplasm (Figure 1A). As expected, SEC31a localized both at the perinuclear region and as punctate cytoplasmic structures, in agreement with previous reports (54). Surprisingly, co-localization between ASO and SEC31a was readily detected. However, not all ASO foci co-localized with SEC31a, and not all SEC31a foci co-stained with ASOs, suggesting that the observed co-localization between ASO and SEC31a was not a staining artifact, e.g. channel cross-talk. Indeed, similar co-localization was observed when using different fluorescent dyes (Supplementary Figure S1A), or using a different SEC31a antibody (Supplementary Figure S1B). Treatment with a SEC31a-specific siRNA reduced the mRNA level and the staining signal intensity (Supplementary Figure S1C and D), validating the specificity of the antibody staining. In addition, ASO-SEC31a co-localization is not unique to this ASO sequence, as four additional PS-MOE gapmer ASOs also showed similar co-localization with SEC31a (Supplementary Figure S2A). Such co-localization is not unique to PS-MOE ASOs, since a 5-10-5 PS-LNA ASO co-localized with SEC31a as well (Supplementary Figure S2B). Furthermore, ASO/SEC31a co-localization was also observed using unlabeled ASOs that were stained with a PS-ASO specific antibody (Supplementary Figure S2C), suggesting the co-localization was not a result of fluorophore labeling of the ASOs, consistent with our previous observations that fluorophore labeled or unlabeled ASOs localized similarly in cells and similarly induced protein re-localization (52,55). However, no substantial co-localization between ASO and SEC31a was detected when one channel (SEC31a) was rotated 90° (Supplementary Figure S2D), indicating that the observed co-localization was not a random coincidence.

To determine whether other COPII coat proteins also co-localize with ASOs, HeLa cells were stained for Sar1, a small GTPase in the inner layer of COPII vesicles. Co-localization was detected between ASO and Sar1 protein (Figure 1B). In addition, Sar1 and SEC31a co-localized with the same ASO foci, when the two proteins were co-stained (Figure 1C). Approximately 36 and 40 co-localization events per cell were observed in this case for ASO/Sar1 and ASO/SEC31a, respectively, as quantified from ∼20 cells (data not shown). ASO/SEC31a/Sar1 co-localization was also confirmed using 3D-imaging (Figure 1D and E; Supplementary Movie S1). These results suggest that ASOs most likely co-localize with COPII vesicles, and not with free SEC31a protein. This view is further supported by the observations that SEC23a or SEC24c, middle layer coat proteins of COPII vesicles, also co-localized with SEC31a in ASO containing foci (Supplementary Figure S3A and B). In addition to HeLa cells, ASO/SEC31a/Sar1 co-localization was observed in A431 cells (Supplementary Figure S4A) and in normal primary human dermal fibroblast cells (HDFn) (Supplementary Figure S4B and C), suggesting that ASO/COPII co-localization was not unique to HeLa cells or to stable cell lines. However, no substantial co-localization was detected between ASO and COPI vesicles, as determined by co-staining of COPI coat proteins ARF1 (Supplementary Figure S5A) or β-COP (Supplementary Figure S5B). These results indicate that COPII vesicles can co-localize with ASOs in cytoplasmic foci. Based on the quality of the antibody for immunofluorescent staining, SEC31a was stained in subsequent studies.

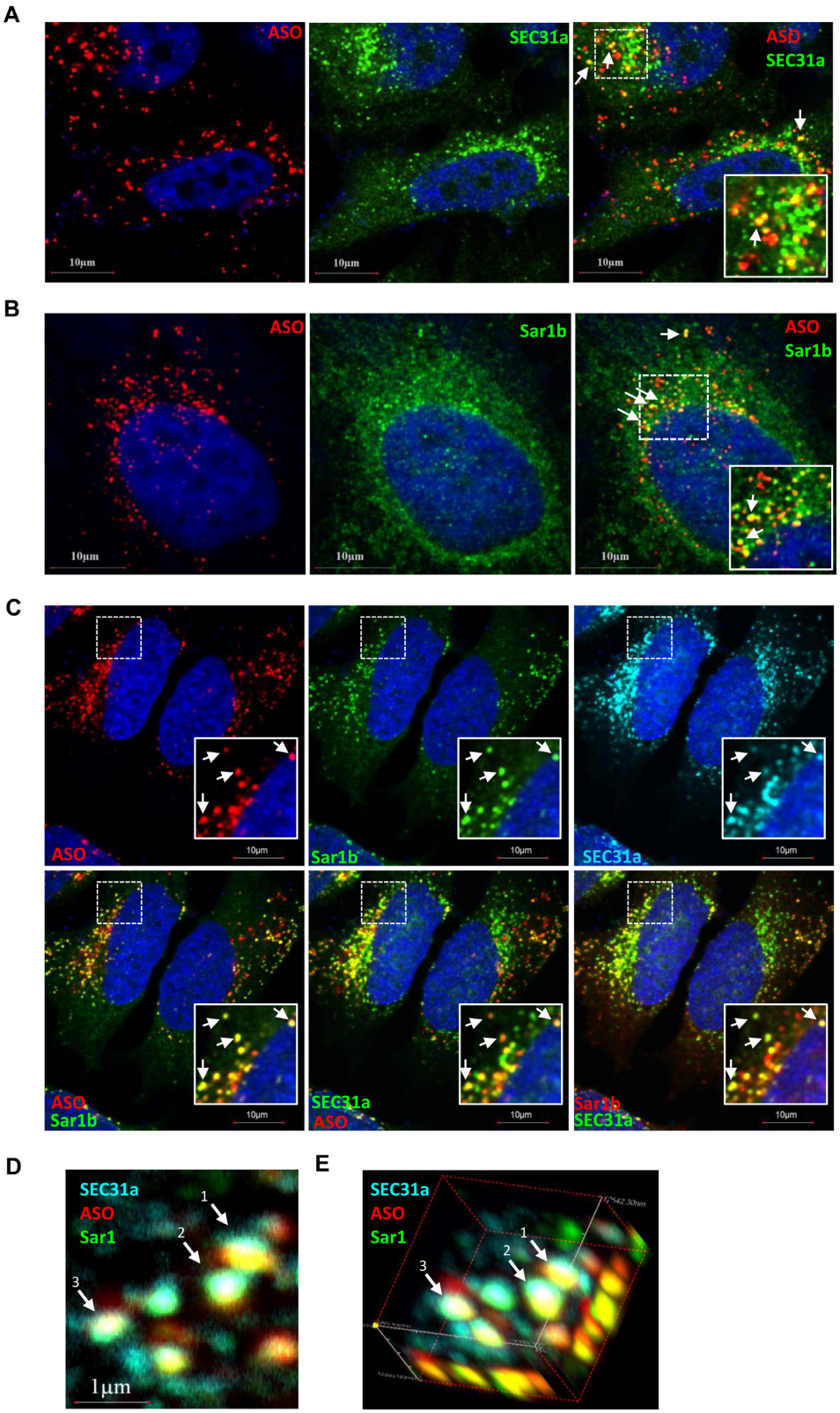

Figure 1. COPII coat proteins can co-localize with ASOs. (**A**) Immunofluorescent staining for SEC31a in HeLa cells incubated with 2 μM ASO446654 for 16 h. (**B**) Immunofluorescent staining for Sar1b in HeLa cells incubated with 2 μM ASO446654 for 16 h. (**C**) Co-staining of SEC31a and Sar1 in HeLa cells incubated with ASOs for 16 h. ASO–protein or protein–protein co-localization is exemplified by arrows. The nucleus was stained with DAPI (blue). ASOs are shown in red. Proteins are shown in green or cyan, as indicated in the figures; scale bars, 10 μm. (**D**) Immunofluorescent staining for SEC31a and Sar1b as in panel (B). Co-localizations are exemplified by arrows. (**E**) 3D-imaging of the same view as in panel (D). The same foci are marked by arrows and numbered as in panel (D).

COPII vesicles co-localize with ASOs in a time dependent manner

Next, the kinetics of COPII vesicle co-localization with ASOs was determined. HeLa cells were incubated with ASOs for different times, and SEC31a was stained (Figure 2A). ASO/SEC31a co-localization was quantified from ∼20 cells (Figure 2B). No substantial co-localization was detected within 4 h after ASO incubation, although significant amount of ASOs has already entered cells. After 6–8 h, SEC31a started to co-localize with ASOs, and such co-localization became more robust after 10 h of ASO incubation. The kinetics of ASO/COPII co-localization correlated with the kinetics of ASO activity, which showed that detectable reduction of the targeted *NCL* or *Drosha* mRNA also occurred between 6 and 8 h after incubation of unlabeled ASOs, as determined using qRT-PCR assay (Figure 2C), consistent with previous reports (9,28). The gapmer ASOs used for activity assays were chosen as they have been well characterized in our previous studies (16,56).

To evaluate whether ASO/COPII co-localization is a dynamic process, HeLa cells were incubated with ASOs for 11, 24, 36 or 48 h, before reaching confluence. Cells were stained with SEC31a (Supplementary Figure S6 and data not shown), and co-localization events were quantified (Figure 2D). The results indicate that ASO/COPII co-localization increased over time and reached highest level at 24–36 h after ASO incubation, then declined. These results suggest that COPII co-localization with ASOs is time dependent and a dynamic process.

COPII vesicles can re-locate to late endosomes upon ASO incubation

It is known that ASOs can migrate from EE to LE within 20–40 min after incubation, and mainly localize to LEs and lysosomes in the cytoplasm after 2 h (28,30). As COPII vesicles co-localized with ASOs at later time points in punctate cytoplasmic structures, it is possible that those structures represent LEs or lysosomes. We thus co-stained SEC31a with LE marker proteins. Without ASO incubation, SEC31a did not substantially co-localize with Rab7 (approximately <2 overlapping per cell) (Supplementary Figure S7A), an LE marker protein, nor with LAMP1 (approximately <4 overlapping per cell) (Supplementary Figure S7B), which stains both LEs and lysosomes, suggesting that under normal conditions, COPII vesicles do not substantially localize to LEs. This was further confirmed in a SVGA cell line stably expressing GFP-Rab7 (Supplementary Figure S7C). No substantial co-localization was detected between Rab7 and stained SEC31a in the absence of ASOs. However, upon ASO incubation, SEC31a was readily found to co-localize with ASOs and with Rab7 in HeLa cells (∼23 overlapping per cell) (Figure 3A) and in GFP-Rab7 expressing SVGA cells (Supplementary Figure S8A–C), indicating that the ASO-positive COPII vesicles co-localize with LEs in different cell types. However, we note that not all ASO-positive COPII vesicles co-localized with Rab7, as exemplified with arrows (Figure 3A-d and A-e), implying that some ASO-containing COPII vesicles may not be present at LEs. In addition, some ASO-positive COPII vesicles partially overlapped with LE (Figure 3A-f, marked with arrowheads), suggesting a possibility that at least some ASO-positive COPII vesicles associated with LE membrane, and not inside LEs. To further confirm this observation, SEC31a was co-stained with LAMP1, which showed a better staining resolution of the limiting membrane of LE/Lysosomes (Figure 3B). Again, some ASO-positive COPII vesicles partially co-localized with the limiting membrane of LAMP1-stained structures (Figure 3B-f). This is more clearly seen in the enlarged image and the signal intensity profile (Figure 3C and D), and by the 3D image (Figure 3E). Although COPII vesicles can co-localize with LEs, no SEC31a was detected to co-localize with ILVs inside LE, even with extensive search (data not shown).

To demonstrate if other molecules taken up by cells through endocytic pathways can also trigger COPII vesicle re-localization to LEs, cells were incubated for 16 h with dextran, a fluid phase marker that can enter cells through macropinocytosis pathway (57). Immunofluorescent staining results showed that, although dextran clearly localized to LEs as previously reported (57), no significant SEC31a co-localization with LE or with dextran was detected (Supplementary Figure S9A). Similarly, SEC31a did not co-localize with Rab7 or with incubated transferrin (Supplementary Figure S9B), which enters the cell via receptor mediated endocytosis (58). These observations indicate that dextran or transferrin incubation did not re-locate COPII to LEs, and that COPII re-localization to LEs is uniquely induced by PS-ASO incubation.

Since ASO incubation can re-locate some COPII vesicles to LEs, we evaluated whether COPII function was affected under these conditions. We analyzed the levels of different groups of proteins in HeLa cells incubated for 24 h with high concentration (10 μM) of ASOs (116847, same as 446654 but without Cy3 dye) (Supplementary Figure S10A). It is known that COPII vesicles are required for ER-to-Golgi transport of many proteins, including membrane and secreted proteins (35). However, ASO incubation did not significantly change the levels of the tested proteins, including cell surface proteins EGFR and LDLR, mitochondria proteins P32 and LRPPRC, Golgi-localized protein STX5, the COPII protein SEC31a, as well as RNase H1, which localizes in mitochondria, cytosol and the nucleus (56). In addition, the levels and patterns of secreted glycoproteins in the medium and in cells were not affected by ASO incubation, as determined by glycoprotein staining (Supplementary Figure S10B, left panel). Furthermore, Coomassie blue staining results indicated comparable levels of total cellular proteins and secreted proteins in the medium with or without ASO incubation (Supplementary Figure S10B, right panel). Moreover, although COPII vesicles are involved in autophagy biogenesis (59), ASO incubation did not substantially induce autophagy in HeLa cells, as indicated by immunofluorescent staining (Supplementary Figure S10C) and western analysis for LC3 (Supplementary Figure S10D), a marker protein of autophagy. No ASO-LC3 co-localization or elevated levels of LC3-II was observed. Together, these results suggest that ASO incubation did not inhibit normal functions of COPII vesicles, likely because only a small portion of COPII vesicles re-located to LEs and the process is dynamic.

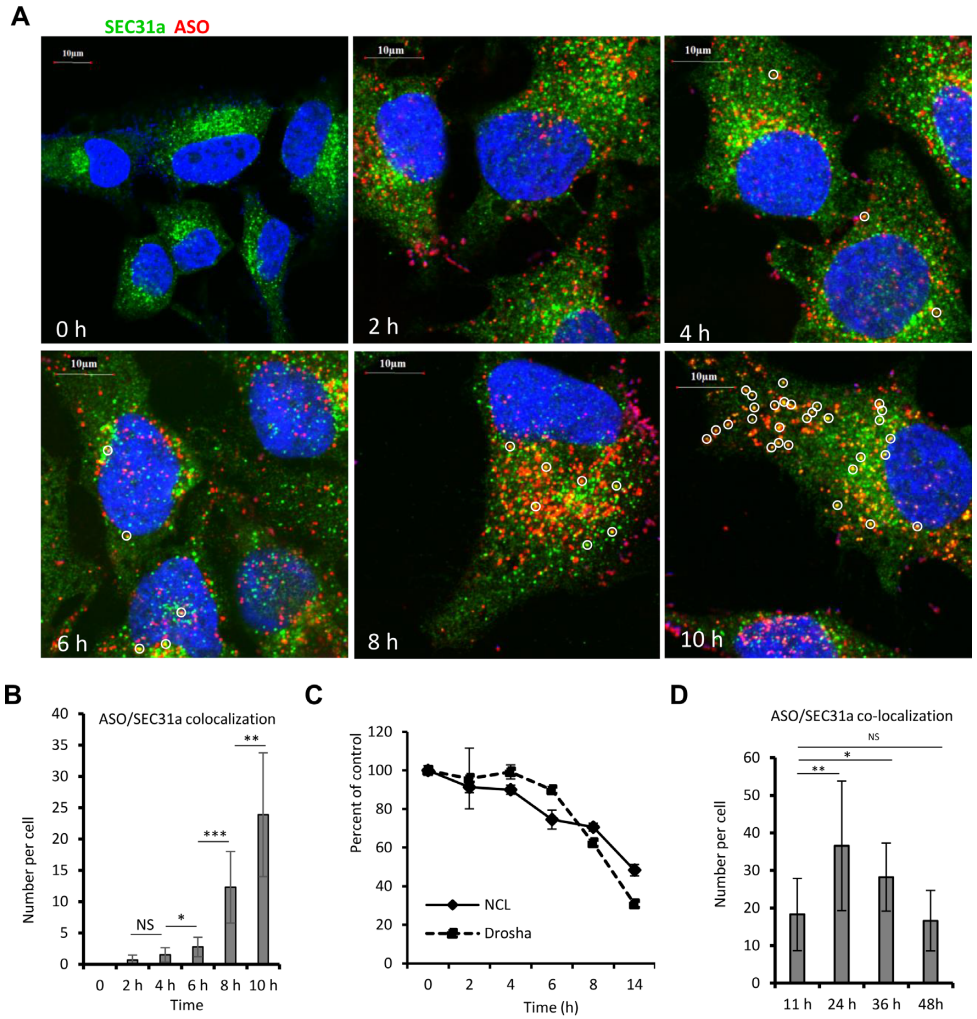

Figure 2. ASO/COPII co-localization is time dependent. (**A**) Staining of SEC31a (green) in HeLa cells incubated with 2 μM ASOs (red) for different times, as indicated. Examples of ASO-SEC31a co-localization are circled; scale bars,10 μm. (**B**) Quantification of ASO/SEC31a co-localization, as detected in panel (A). *P*-values were calculated based on unpaired *t*-test using prism. (**C**) qRT-PCR quantification for the levels of *NCL* and *Drosha* mRNAs in cells incubated for different times with 10 μM *NCL*-targeting ASO110080 or *Drosha*-targeting ASO25960. The error bars represent standard deviations from three independent experiments. (**D**) Quantification of ASO/COPII co-localization in HeLa cells incubated with 2 μM ASOs for different times, as indicated. Error bars are standard deviations of co-localization events counted from 20 cells in each case. *P*-values were calculated based on unpaired *t*-test using prism. NS, not significant; *, P<0.05; **, P<0.01; ***, P<0.001. We note that the experiments were performed three times and similar trends were observed.

Reduction of COPII proteins decreased ASO activity

The re-localization of COPII vesicles to LEs upon ASO incubation suggests that COPII vesicles may affect ASO activity, particularly as the onset of ASO activity appeared to be roughly at the same time as the ASO/COPII co-localization. To evaluate this possibility, SEC31a and the two isoforms of SEC23 proteins (SEC23a and SEC23b) were reduced in HeLa cells by siRNA treatment (Figure 4A), followed by incubation with unlabeled ASOs targeting different RNAs. qRT-PCR analyses showed that reduction of either SEC23 or SEC31a protein decreased the activities of the ASOs targeting *NCL* or *Drosha* mRNAs (Figure 4B and C). We note that this and subsequent activity assays were performed more than three times with similar observations, and were also confirmed with different siRNAs (data not shown). Only representative results are presented.

Next, we determined if the observed effects of reduction of COPII proteins on ASO activity are unique to HeLa cells. We attempted several times without success in primary HDFn cells, due to extremely low siRNA transfection efficiency and lack of ASO activity upon free uptake in these cells (data not shown), which is not surprising as many cell lines do not exhibit ASO activity upon free uptake, such as HepG2 cells. We then evaluated the effects of COPII proteins in A431 cells, which exhibit robust ASO activity upon free uptake (28). SEC31a and the two isoforms of Sar1 proteins were reduced by siRNA treatment (Figure 4D). Reduction of the coat proteins in these cells also decreased the antisense activities of ASOs targeting *NCL* (Figure 4E), *Drosha* (Figure 4F and G) or Malat1 RNA (Figure 4H). Furthermore, reduction of two additional COPII coat proteins, SEC13 and SEC23, also reduced ASO activity in A431 cells (Supplementary Figures S11A and B). However,

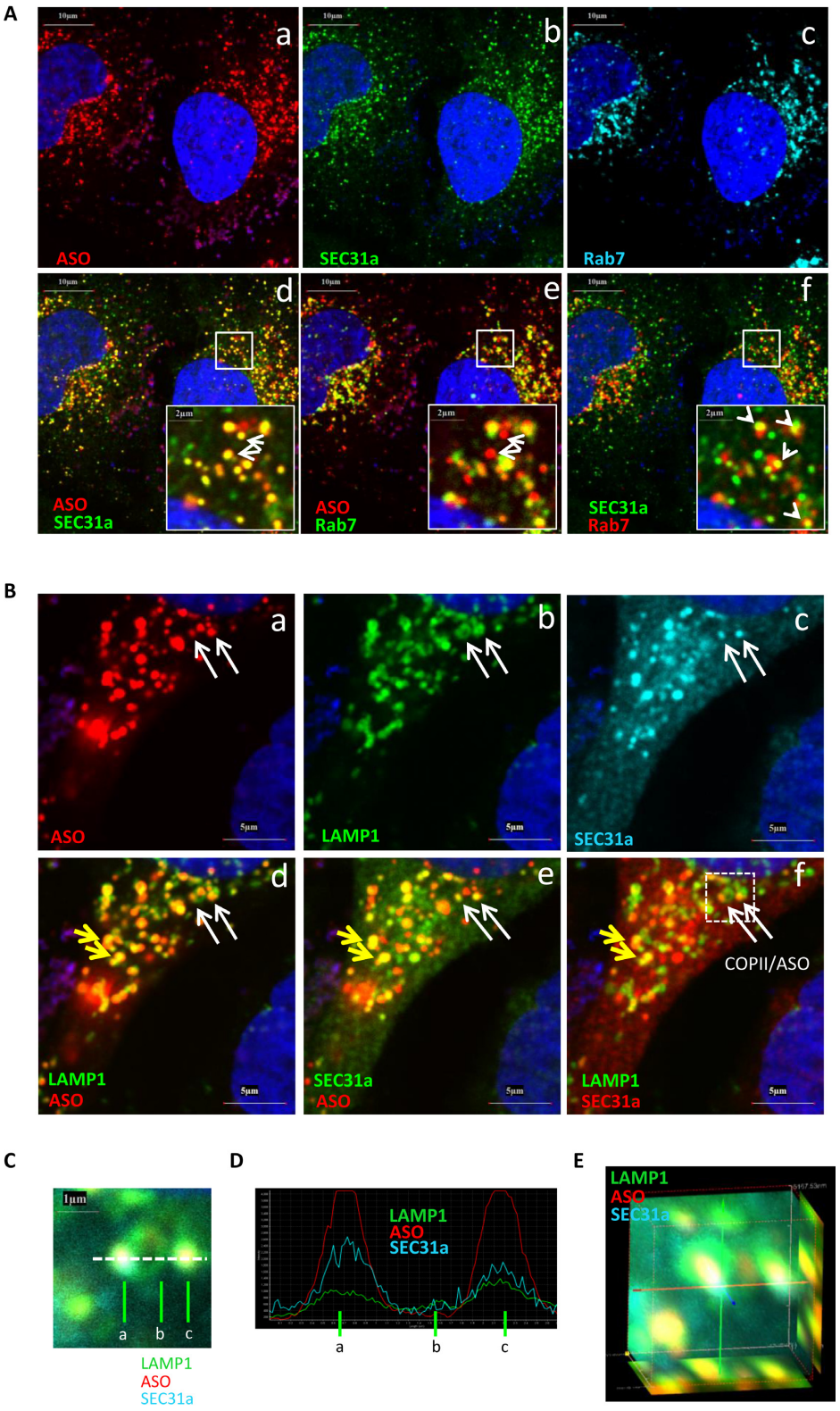

Figure 3. COPII vesicles can co-localize with ASOs at LEs. (**A**) Immunofluorescent staining of SEC31a and Rab7 in HeLa cells incubated with 2 μM ASOs for 16 h. Nucleus was stained with DAPI; scale bars, 10 μm. (**B**) Co-staining of SEC31a and LAMP1 in HeLa cells incubated with ASOs as above. Yellow arrows exemplify SEC31a overlapping with LAMP1-stained foci. White arrows indicate COPII/ASO foci partially overlapping with the limiting membranes of LAMP1-stained foci; scale bars, 5 μm. The boxed region was enlarged and Z-section image was taken, as shown in panels (**C**), (**D**) and (**E**), using the same color code. (C) An enlarged image area as boxed in Figure 3B-f. The dashed line indicates the section used to analyze signal intensity profile, as shown in panel (D). The LAMP1 staining boundaries of one organelle (a,b) and the center of another organelle (c) are indicated. (E) A 3D image for the enlarged foci.

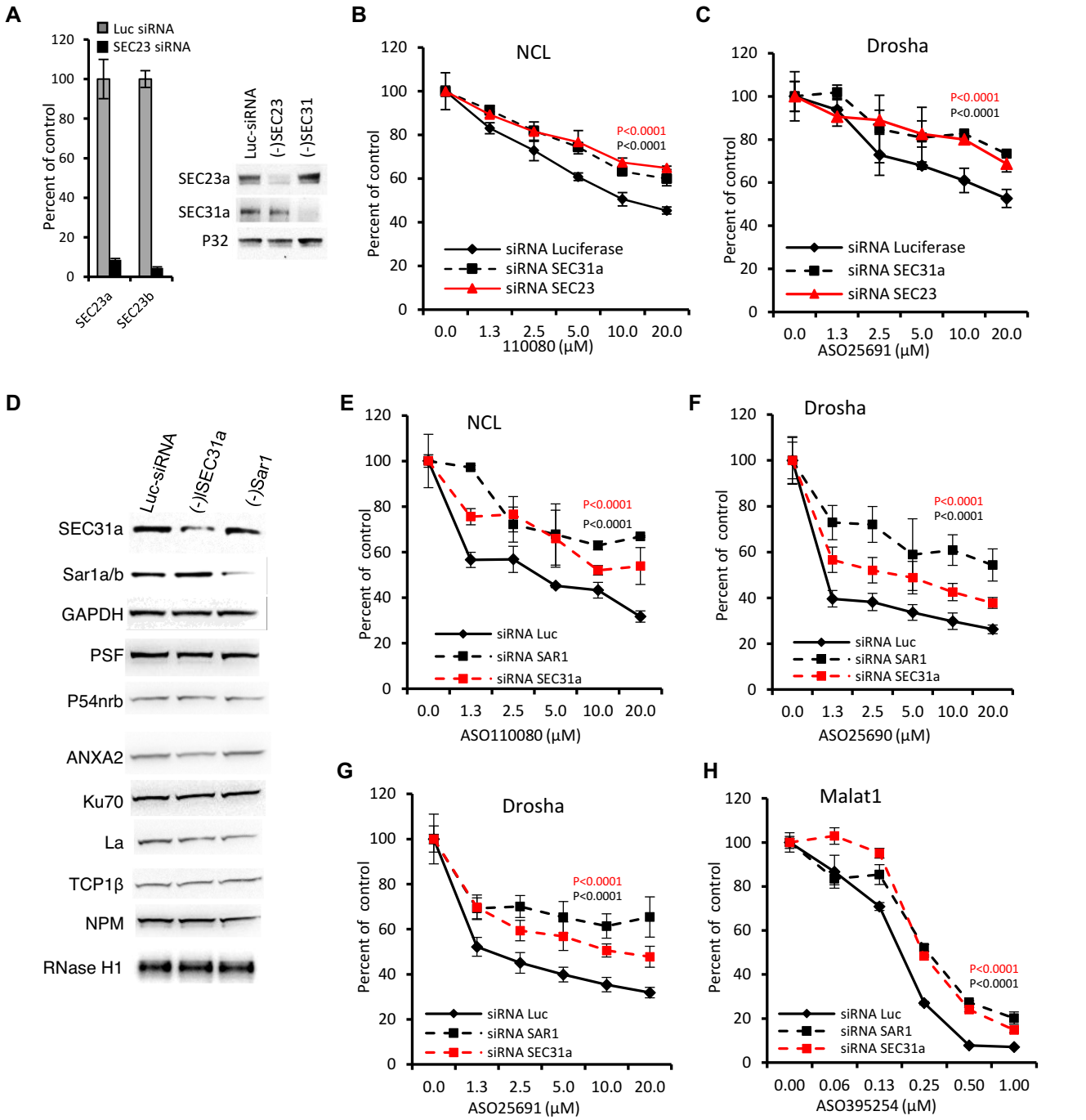

Figure 4. Reduction of COPII coat proteins decreased ASO activity. (**A**) Reduction of SEC23 and SEC31a proteins in HeLa cells treated with siRNAs for 72 h. Left panel, qRT-PCR quantification for the levels of two isoforms of *SEC23*. Right panel, western analyses for SEC23a and SEC31a proteins. P32 was as a control for loading. (**B**) qRT-PCR quantification for the levels of *NCL* mRNA in siRNA-treated HeLa cells that were incubated with ASO for overnight. (**C**) qRT-PCR quantification for the levels of *Drosha* mRNA, as in panel (B). (**D**) Western analyses of the levels of SEC31a and Sar1 proteins in A431 cells treated with siRNAs for 72 h. Sar1 was detected using an antibody that recognizes both isoforms (07-692, Millipore). The levels of other proteins known to be important for ASO activity were also determined. GAPDH was served as a control for loading. The siRNA-treated A431 cells were incubated for overnight with different ASOs targeting *NCL* (panel (**E**)), *Drosha* (**F** and **G**), or Malat1 (**H**) RNAs. The levels of the targeted RNAs were determined by qRT-PCR. The error bars represent standard deviations from three independent experiments. *P*-values were calculated with *F*-test using Prism.

reduction of ARF1, a COPI vesicle protein that did not co-localize with ASOs, had no significant effect on ASO activity, as tested in A431 cells (Supplementary Figures S11C–E) and in HeLa cells (data not shown). Together, these results indicate that reduction of various COPII coat proteins can decrease ASO activity in different cells.

The effect of COPII proteins on ASO activity is mediated by endocytic pathways

To achieve antisense activity, internalized ASOs need to be released from membrane-enclosed endocytic organelles to the cytosol and nucleus, where ASOs can hybridize to target RNAs and recruit RNase H1 for cleavage (9,56). Thus, ASO activity can be affected at different stages, e.g. before or after release from endocytic organelles. As COPII vesicles are required for transport of many proteins during their biogenesis, reduction of COPII coat proteins may unexpectedly affect the levels of proteins important for ASO activity after release, leading to decreased ASO activity. For examples, we previously found that some cellular proteins, e.g. PSF, P54nrb, TCP1, Ku70, La or NPM1 (13,52,60), can affect ASO activity upon transfection, which bypasses normal endocytic and release pathways and delivers ASOs largely to the cytosol and the nucleus. However, results of western blots showed that under the experimental conditions, reduction of SEC31a or Sar1 did not affect the levels of these proteins or RNase H1 (Figure 4D), implying that reduction of COPII proteins may not affect ASO activity once ASOs are released from endocytic organelles. Indeed, this is supported by the observations that reduction of Sar1 or SEC31a as in Figure 4D–H did not impair ASO activity upon transfection (Supplementary Figure S12A and B).

Although COPII vesicles are required for transport of many proteins out of ER, under the experimental conditions we used, reduction of COPII coat proteins did not cause ER stress, as the level of phosphorylated eIF2a protein was not significantly altered (Supplementary Figure S13A). In addition, even induction of ER stress by thapsigargin treatment did not substantially alter ASO activity (Supplementary Figure S13B and C), indicating that the altered ASO activity upon COPII protein reduction did not stem from ER stress. Altogether, these results suggest that COPII vesicles are important participant in productive trafficking of ASOs and that the effects of reduction of COPII proteins on ASO activity must occur during or before release of ASOs from endocytic organelles.

Reduction of COPII protein can decrease ASO release from late endosomes

Next, we analyzed the effects of reduction of COPII coat proteins on ASO endocytic trafficking. Even though COPII vesicles are required for transport of secreted and membrane proteins, reduction of Sar1 or SEC31a did not reduce the levels of ASO uptake, as determined by flow cytometry using Cy3-labeled ASOs incubated with HeLa cells for 3 h (Figure 5A and B). This result suggests that under our experimental conditions, surface proteins important for ASO uptake may not be substantially affected by reduction of the COPII proteins. This is supported by the observations that reduction of SEC31a did not substantially alter the surface localization pattern and the signal intensity of EGFR protein (Supplementary Figure S14A), which normally localizes in plasma membranes and is associated with productive ASO trafficking and activity (21). In addition, the ASO localization pattern and signal intensity also appear comparable at 2 h after incubation between control and SEC31a reduced cells (Supplementary Figure S14B), suggesting that ASO transport to LE/Lysosome was not inhibited, since 2 h after incubation ASOs had already passed through EE and were mainly localized in LE/Lysosomes (28,30).

To further determine whether ASO trafficking from EE to LE is affected by reduction of SEC31a, ASOs were incubated with HeLa cells for 20 or 40 min, early time points at which ASOs have entered EE and LE (28). Cells were stained for EE marker protein EEA1 and LE marker protein Rab7 (Supplementary Figure S14C and D). Quantification of ASO-positive EEs and LEs showed that reduction of SEC31a did not substantially affect ASO transport from EE to LE, as comparable levels of ASO-positive EEs or LEs were observed between control and SEC31a reduced cells at these time points (Figure 5C). In addition, SEC31a did not co-localize with ASOs in EEs at these times in control cells (Supplementary Figure S14C and data not shown), consistent with later co-localization between ASO and COPII as described above. Together, these results indicate that ASO uptake and transport to LE were not impaired by reduction of SEC31a.

Next, we analyzed whether ASO release from LEs was affected by COPII reduction. HeLa cells were incubated with an unlabeled ASO targeting *Drosha* mRNA for 2 h to ensure sufficient uptake of ASOs to achieve antisense activity. Medium was then changed to remove ASOs thus to eliminate further uptake (Figure 5D, upper panel), as we described previously (28,30). Cells were collected at different times after ASO removal and the levels of targeted *Drosha* mRNA was determined by qRT-PCR (Figure 5D, lower panel). The results showed that reduction of SEC31a decreased ASO activity under these conditions. As ASO uptake is not affected by SEC31a reduction and internalized ASOs can pass through EE and enter LE within 1–2 h (28,30), the decreased ASO activity after ASO removal should mainly reflect reduction of ASO release from LEs. These results together suggest that reduction of COPII coat protein decreased ASO release from endocytic organelles.

ASO incubation can induce the recruitment of pre-assembled COPII vesicles to LEs

Co-localization between ASO and COPII vesicles at LE may occur through different pathways. For example, released ASOs on the cytosolic side of LE may interact with the surface components of COPII vesicles; COPII vesicles may contact ASO-containing LEs, or ASOs may be loaded into COPII vesicles during vesicle assembly at ER and subsequently re-localize to LEs. To distinguish between these possibilities, we first determined whether ASOs can bind to the core coat proteins. Affinity selection was performed using a biotinylated PS-ASO and bound proteins were eluted by competition using non-biotinylated ASOs, as we reported previously (52). Western analyses showed that none

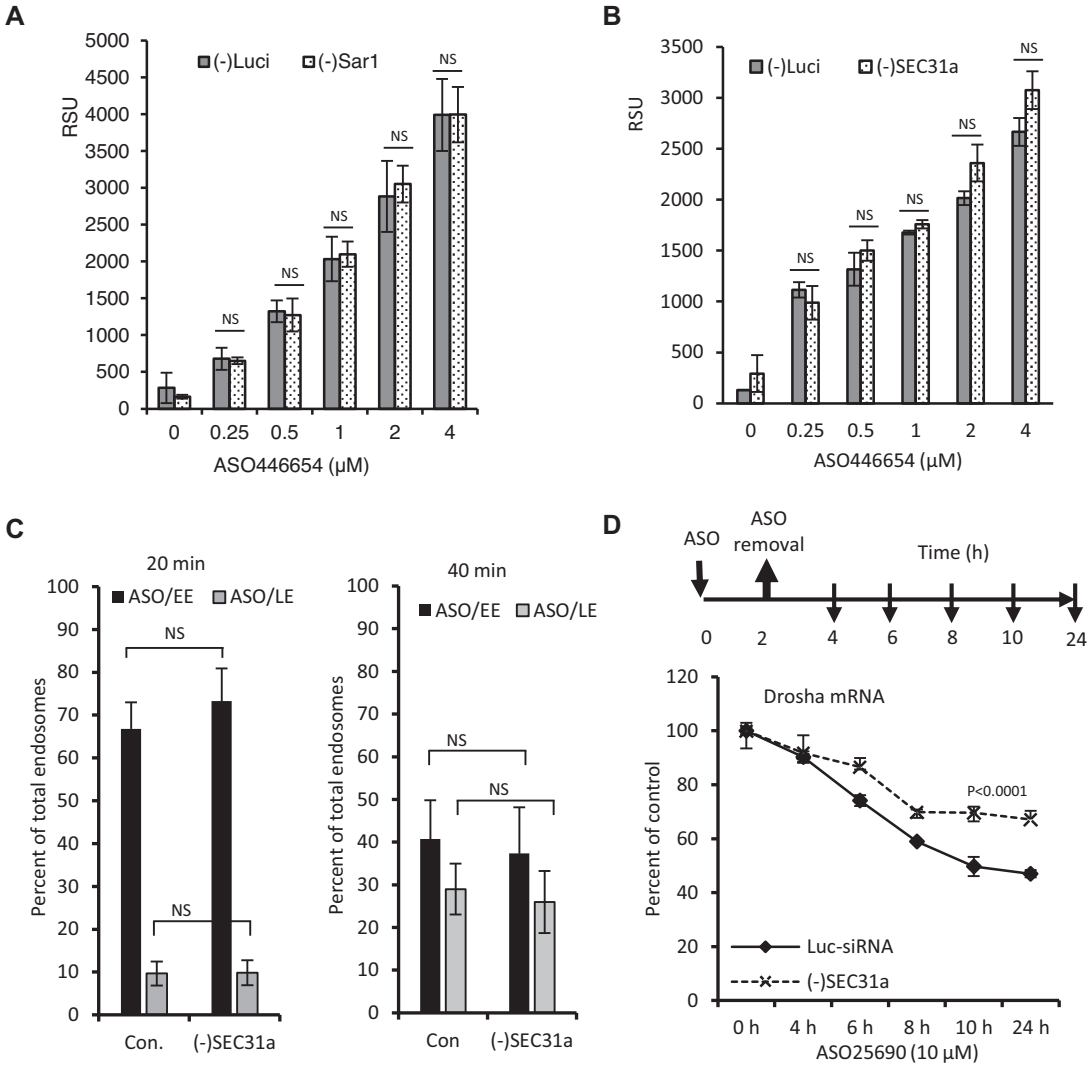

Figure 5. Reduction of COPII coat proteins can impair ASO release from endocytic pathways. (**A**) Flow cytometry analysis of the levels of ASO uptake in control or *SAR1* siRNA-treated HeLa cells. (**B**) Flow cytometry analysis of the levels of ASO uptake in control or *SEC31a* siRNA-treated HeLa cells; RSU, relative fluorescence unit. The error bars represent standard deviations from three independent experiments. *P*-values were calculated using unpaired *t*-test. (**C**) quantification of ASO localization to EE or LE at 20 or 40 min after ASO incubation in HeLa cells treated with different siRNAs. The error bars represent standard deviations of the results counted from 20 cells in each case. *P*-values were calculated using unpaired *t*-test**.** (**D**) Reduction of SEC31a decreased ASO activity when ASO uptake was terminated early. Upper panel indicates the procedure of ASO incubation, removal and time points for cell harvest. Lower panel indicates the qRT-PCR quantification of *Drosha* mRNA in HeLa cells incubated with ASOs for different times. The error bars represent standard deviations from three independent experiments. *P*-values were calculated with *F*-test using Prism.

of the five core coat proteins was co-isolated with PS-ASOs (Supplementary Figure S15A), whereas a known ASO-binding protein, Ku80, was effectively co-isolated (13). This observation was further confirmed using a more sensitive approach, the BRET binding assay that we recently developed (53). The binding between ASO and Sar1, or between ASO and SEC13, appeared to be weak, with a k_d above the highest concentration tested (>3 μM) (Supplementary Figure S15B), whereas the k_d for many ASO-binding proteins were detected in the low nanomole range (53). Although it is possible that additional COPII-associated proteins may interact with released cytosolic ASOs, this seems unlikely, since upon transfection, with which ASOs were largely released to the cytosol and the nucleus (61), no ASO/COPII co-localization was detected (Supplementary Figure S15C). Together, these results argue against the possibility that released ASOs associate with the surface of COPII vesicles.

Next, we determined whether COPII vesicles associated with ASOs before re-localization to LEs. One possibility is that ASO/COPII association occurs at EE during endocytic trafficking. However, no COPII/EE co-localization was detected when ASOs localized to EEs at early times after ASO incubation (Supplementary Figures S14C and S15D), or at later times when ASO/COPII co-localization occurred (Supplementary Figure S15E). These results imply that ASO/COPII association may not occur at EE. Next, we analyzed if ASO/COPII association occurred during COPII vesicle assembly and/or transport from ER to Golgi. We reasoned that if ASO and COPII associate during COPII assembly, ASOs might be detected at ERES

where COPII assembly occurs. However, co-localization was not detected between ASOs and SEC16, an ERES marker protein (42), although ASOs could co-localize with SEC31a in cytoplasmic foci lacking SEC16 (Figure 6A, white arrows), and SEC31a could co-localize with SEC16 at ERES without ASO (yellow arrows). These results indicate that ASO/COPII co-localization does not occur at ERES. In addition, upon ASO incubation, COPII vesicles could reach ERGIC, as indicated by the co-localization between SEC31a and ERGIC-53 (Supplementary Figure S16A and B), consistent with previous reports (62). However, ERGIC-localized COPII did not contain ASO (dashed circle), and ASO-containing COPII did not co-localize with ERGIC (solid circle) (Supplementary Figure S16A and B), further suggesting that ASO/COPII association did not occur during COPII assembly on ER or during transport from ER to ERGIC.

The above observations suggest the possibility that ASO/COPII co-localization at LE does not require *de novo* formation of COPII vesicles, rather, budded COPII vesicles that have already exited the ER may contact LE to co-localize with ASOs and to affect ASO activity. To evaluate this possibility, we reduced SEC12 (Figure 6B), which is required for the initiation of COPII assembly on ER (36,63). Reduction of SEC12 by siRNA treatment for 72 h did not abolish ASO/COPII co-localization (Figure 6C) and did not inhibit ASO activity (Figure 6D). Similarly, reduction of SEC16A, another protein involved in COPII assembly (42,64), did not abolish ASO/COPII co-localization 72 h after siRNA treatment (Supplementary Figure S17A and B). Consistently, ASO activity was also not affected at this time point by reduction of SEC16A in both HeLa (Supplementary Figure S17C) and A431 cells (Supplementary Figure S17D and E). These results further suggest that ASO/COPII co-localization at LE does not require *de novo* assembly of COPII vesicles at ERES. However, reduction of SEC16A in HeLa cells for a longer time (96-h siRNA treatment) decreased ASO activity (Supplementary Figure S17F and G) and ASO/SEC31a co-localization (Supplementary Figure S17H and I), implying that blocking COPII assembly ultimately reduced the levels of functional, pre-assembled COPII vesicles. In addition, treatment for 8 h with brefeldin A (BFA), an inhibitor for ER–Golgi transport, did not abolish ASO/COPII co-localization at LEs (Supplementary Figure S18), although COPII vesicles became scattered in the cytoplasm in BFA-treated cells, as compared with the perinuclear localization pattern in control cells, consistent with previous observations (65). By contrast, treatment for 1 h with chloroquine, an endosome/lysosome disruption agent that inhibits endosomal acidification, significantly impaired ASO/COPII co-localization (Figure 6E). Altogether, these results strongly suggest that pre-assembled COPII vesicles can re-locate to LE upon ASO incubation, where they co-localize with ASOs.

STX5 re-localizes to LE upon ASO incubation

Next, we sought to demonstrate what factors might be required for COPII re-localization to LE. It is possible that some other proteins also re-locate to LE upon ASO incubation and are required for COPII re-localization to LE. Although ANXA2 can re-locate to LE upon ASO incubation and affects ASO activity as we reported previously (13), reduction of ANXA2 did not affect ASO/COPII co-localization at LEs (data not shown). On the other hand, P115 has been shown to be involved in docking of COPII vesicles to the Golgi membrane, and COPII fusion with the Golgi membrane requires STX5, an ER–Golgi SNARE protein (47–51). We thus determined whether P115 and STX5 were recruited to LE upon ASO incubation. In control HeLa cells, P115 and STX5 mainly localize at Golgi (Supplementary Figure S19A), as previously reported (66,67). However, after ASO incubation, STX5 and not P115, substantially co-localized with ASOs in punctate cytoplasmic foci (Supplementary Figure S19B). ASO/STX5 colocalization was further confirmed using unlabeled ASOs (Supplementary Figure S19C). In addition, ASO/STX5 co-localization was also observed in A431 cells (Supplementary Figure S20).

To ascertain if STX5 co-localizes with COPII vesicles, HeLa cells were co-stained with STX5 and SEC31a. Without ASO incubation, co-localization between STX5 and SEC31a can be occasionally detected in small, punctate cytoplasmic structures, as indicated by arrows (Figure 7A). However, upon ASO incubation, some scattered STX5 foci appeared to be slightly larger and co-localized with both SEC31a and ASO (Figure 7B), although smaller STX5/SEC31a co-localization foci lacking ASO could still be detected (marked with yellow arrows). ASO/COPII/STX5 co-localization was also observed in primary HDFn cells by co-staining of STX5 and Sar1 (Supplementary Figure S21). In addition, chloroquine treatment significantly abolished both SEC31a and STX5 co-localization with ASOs (Figure 7C). These observations suggest that some STX5 was recruited to LE upon ASO incubation, as SEC31/ASO mainly co-localized at LEs. This view was confirmed by co-staining of STX5 and Rab7 in HeLa cells. Although STX5 was not co-localized with Rab7 in control cells without ASO treatment (Supplementary Figure S22A), substantial re-localization of STX5 to ASO-containing LEs was observed upon ASO incubation (Supplementary Figure S22B) and was confirmed using 3D-imaging (Supplementary Figure S22C). Additionally, STX5/ASO co-localization with GFP-Rab7 was also detected in SVGA cells (Supplementary Figure S22D). Furthermore, ASO/STX5 co-localization appeared at similar times with that of ASO/COPII co-localization, as determined by co-staining of STX5 and SEC31a in HeLa cells incubated with ASOs for different times (Figure 7D and Supplementary Figure S23).

Reduction of STX5 and P115 decreased ASO activity and ASO/COPII co-localization

To determine if STX5 and P115 affect ASO activity, A431 cells were treated with corresponding siRNAs, which specifically reduced the levels of two forms of STX5 derived from alternative translation (68) (Figure 8A), and the P115 protein (Figure 8D). Reduction of STX5 or P115 significantly decreased ASO activities, as demonstrated using unlabeled ASOs targeting different RNAs (Figure 8B–F). Similarly,

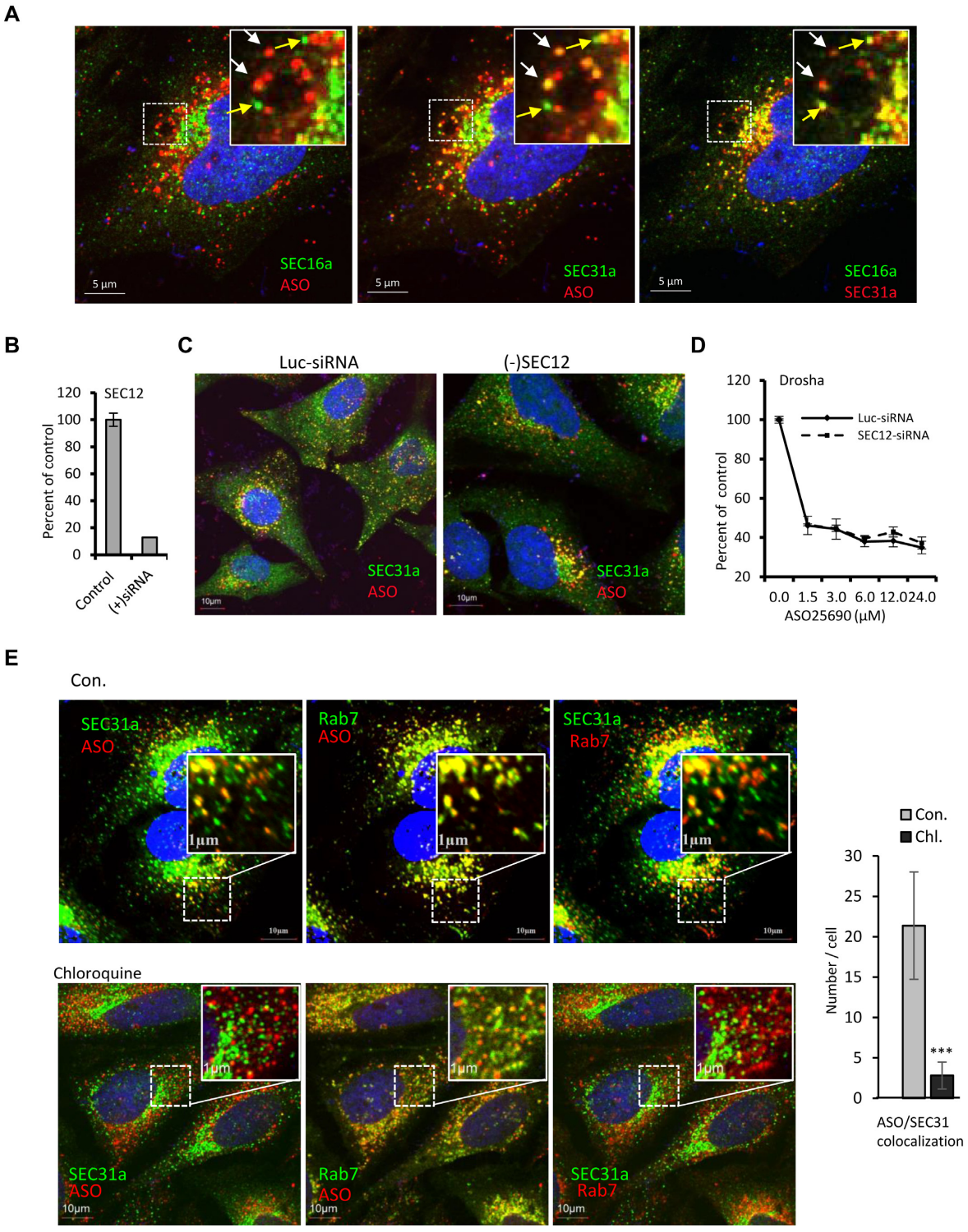

Figure 6. COPII/ASO co-localization does not require *de novo* COPII assembly at ERES. (**A**) Immunofluorescent staining of SEC16a and SEC31a in HeLa cells incubated with 2 μM ASO446654 for 16 h. ASO/SEC31a co-localization is indicated with white arrows, whereas SEC16a/SEC31a co-localization is marked with yellow arrows. (**B**) qRT-PCR quantification for the level of *SEC12* mRNA in HeLa cells treated with luciferase siRNA (control) or *SEC12* specific siRNA [(+)siRNA]. (**C**) Immunofluorescent staining of SEC31a in siRNA-treated HeLa cells incubated with 2 μM ASO446654 for 16 h. (**D**) qRT-PCR quantification for the levels of *Drosha* mRNA in siRNA-treated HeLa cells incubated with ASOs. The error bars represent standard deviations from three independent experiments. (**E**) Immunofluorescent staining of SEC31a and Rab7 in HeLa cells incubated with 2 μM ASOs for 16 h, followed by treatment with control DMSO for 1 h (upper panel), or with 100 μM chloroquine for 1 h (lower panel); scale bars, 10 μm. ASO/SEC31a co-localization events were quantified and plotted in right panel. *P*-value was calculated based on unpaired *t*-test. ***, P<0.001.

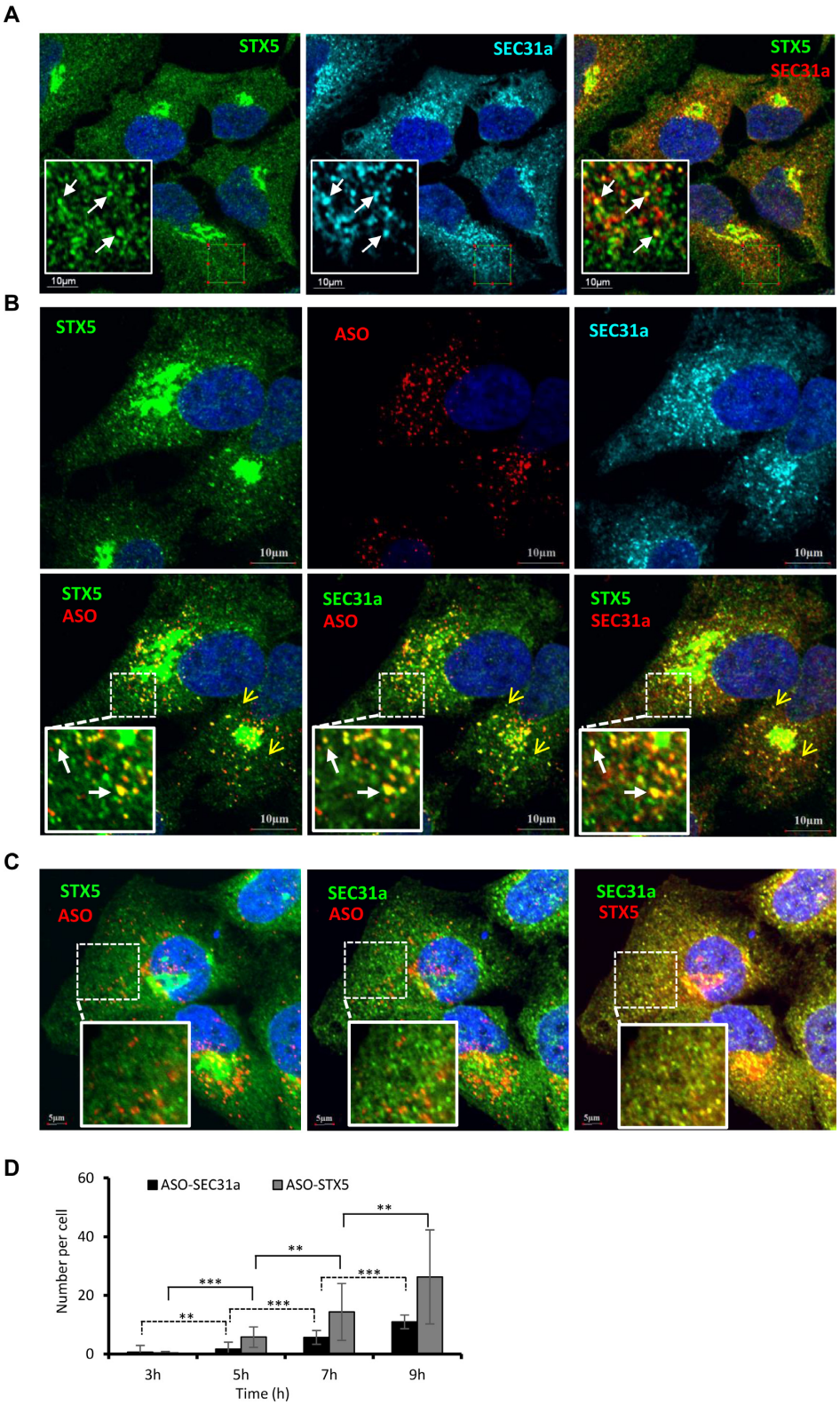

Figure 7. STX5 can re-locate to LEs upon ASO incubation. (**A**) Co-staining of STX5 and SEC31a in HeLa cells without ASO incubation. Occasional co-localization in scattered cytoplasmic foci is marked with arrows. (**B**) Co-staining of STX5 and SEC31a in HeLa cells incubated with 2 μM ASO446654 for 16 h. STX5/SEC31a/ASO co-localization is marked with white arrows in the enlarged images, whereas ASO negative STX5/SEC31a co-localization is exemplified with yellow arrows; scale bars, 10 μm. (**C**) Co-staining of STX5 and SEC31a in HeLa cells treated with 2 μM ASO446654 for 16 h, following by treatment with chloroquine for an additional 1 h; scale bars, 5 μm. (**D**) Quantification of ASO/STX5 and ASO/SEC31a co-localization at different times after ASO incubation in HeLa cells. Error bars indicate standard deviations of co-localization events as counted in 20 cells in each case. *P*-values were calculated using unpaired *t*-test. **, $P<0.01$; ***, $P<0.001$.

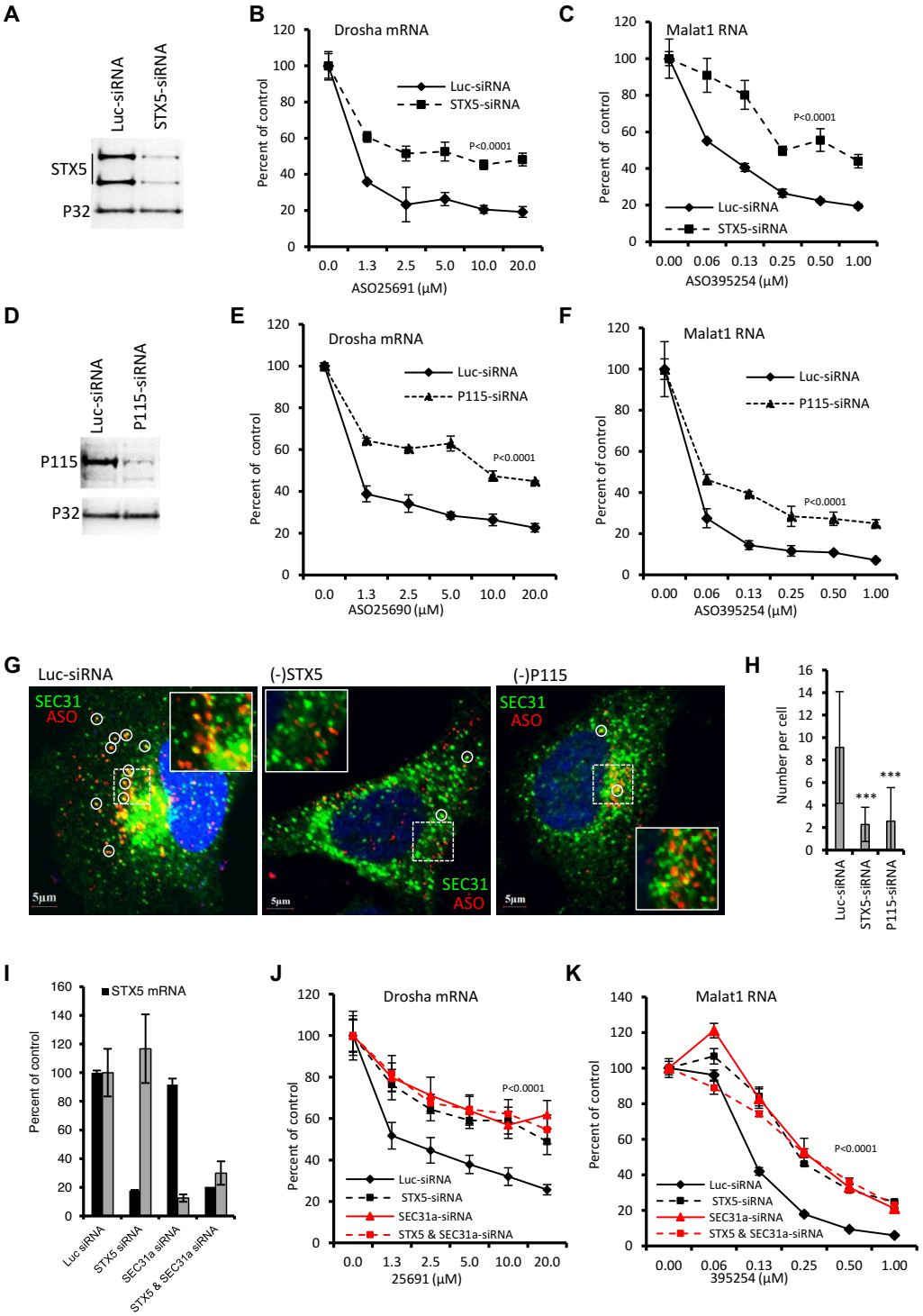

Figure 8. Reduction of STX5 and P115 reduced ASO Activity and ASO/COPII co-localization. (**A**) Western analysis for the levels of STX5 proteins in A431 cells treated with different siRNAs. P32 was served as a control for loading. Control or STX5-reduced cells were incubated with ASOs targeting *Drosha* mRNA (**B**) or Malat1 RNA (**C**), and the levels of the targeted RNAs were analyzed using qRT-PCR. (**D**) Western analysis for the levels of P115 in siRNA-treated A431 cells. P32 was served as a control for loading. Control or P115-reduced cells were incubated with ASOs targeting *Drosha* (**E**) or Malat1 (**F**), and the levels of the targeted RNAs were analyzed using qRT-PCR. The error bars represent standard deviations from three independent experiments. (**G**) Immunofluorescent staining of SEC31a in HeLa cells treated with different siRNAs for 56 h, followed by incubation with 2 μM ASO446654 for an additional 16 h. The co-localization between ASO and SEC31a is marked with circle; scale bars, 5 μm. (**H**) Quantification of ASO/COPII co-localization in HeLa cells treated with different siRNAs as in panel (G). Error bars indicate standard deviations of co-localization events as counted in 20 cells in each case. *P*-values were calculated using *F*-test except panel (H), which was calculated using *t*-test; $***P < 0.001$. (**I**) qRT-PCR quantification for the levels of mRNAs in A431 cells treated with different siRNAs. (**J**) qRT-PCR quantification for the levels of *Drosha* mRNA in different test cells treated with ASO25691 for overnight. (**K**) qRT-PCR quantification for the levels of Malat1 RNA in different test cells treated with ASO395254 for overnight. The error bars represent standard deviations from three independent experiments. *P*-values were calculated using *F*-test with Prism.

reduction of these two proteins also reduced ASO activity in HeLa cells (Supplementary Figure S24A–C). To exclude the possibility that the effect of STX5 reduction on ASO activity is a general effect of Golgi-localized syntaxin proteins, we tested STX6 and STX16, two other SNARE proteins that are involved in retrograde transport between endosomes and Golgi (69–72). Both STX6 and STX16 were localized to Golgi as expected (Supplementary Figure S25A and B), and co-localization between ASO and STX6, and not STX16, could be observed (Supplementary Figure S25A). However, reduction of either protein did not affect ASO activity (Supplementary Figure S25C–E) and ASO/COPII co-localization (Supplementary Figure S25F and G). These results suggest that STX5 and P115 may have specific roles in mediating ASO activity, most likely through their involvement in COPII-mediated pathways.

Next, the effects of reduction of STX5 and P115 on ASO/COPII co-localization were determined.

HeLa cells treated with siRNA targeting STX5 or P115 were incubated with ASOs and SEC31a was stained. Reduction of STX5 or P115 led to a more scattered distribution of SEC31a stained foci (Figure 8G and data not shown), whereas in control cells SEC31a tended to localize to the perinuclear region, consistent with previous studies and their roles in tethering and fusion of COPII vesicles with Golgi membranes (47–51,73). Reduction of STX5 or P115 also decreased the ASO/COPII co-localization, as compared with that in control cells (Figure 8G and H, data not shown). On the contrary, reduction of SEC31a did not abolish STX5/ASO co-localization (Supplemental Figure S26), suggesting that STX5 re-localization to LE is necessary but not sufficient to ensure ASO activity. Together, these results showed that reduction of P115 and STX5 impaired both ASO activity and ASO/COPII co-localization.

To evaluate whether STX5 affected ASO activity through altering the same pathway as COPII vesicles, STX5 and SEC31a proteins were reduced by siRNA treatment either individually or simultaneously. We reasoned that if the effects of STX5 and COPII vesicles on ASO activity resulted from different pathways, additive effects should be expected when these proteins are simultaneously reduced. However, the results indicate that simultaneous reduction of both STX5 and SEC31a decreased ASO activity to an extent similar to that of reduction of either individual protein (Figure 8I–K). Altogether, these data suggest that STX5 affects ASO activity most likely by affecting the same pathway as COPII vesicles, and that STX5 may act at a step preceding ASO/COPII co-localization.

STX5 re-localization to LEs is likely mediated by ASO–protein interactions

Next, we attempted to determine what factor(s) is required for STX5 re-localization to LEs upon ASO incubation. Although the coat proteins of COPII vesicles do not interact with PS-ASOs, STX5 was found to be able to bind PS-MOE ASO (Figure 9A), as determined using the affinity selection assay (52). This observation raises a possibility that STX5 re-localization to LE might be mediated by ASO–protein interactions. To evaluate this possibility, five 20-mer deoxyoligonucleotides were synthesized that share the same sequence as ASO446654 but with different numbers of PS moieties, as protein binding is significantly affected by the numbers of continuous PS backbone (11,52). As expected, reduction of the PS numbers decreased the binding affinity of the ASOs with STX5, and no binding was observed for the ASO with PO backbone (Figure 9B) as determined using the BRET binding assay (53).

To demonstrate the effects of PS numbers on ASO/STX5 co-localization, the five ASOs with different PS numbers were conjugated with Cy3, and incubated with HeLa cells. STX5/ASO co-localization was also dramatically decreased when the PS number of ASOs was reduced, and no substantial co-localization was detected when the PS number was below 11 (Figure 9C and D). This ASO/STX5 co-localization correlates with the ASO/STX5 binding, supporting the hypothesis that recruitment of STX5 to LEs is mediated via ASO–protein interactions.

To further confirm this observation and to exclude the potential influence of PS numbers on ASO uptake, a 5-10-5 PS-MOE ASO and a 5-10-5 PO-MOE ASO were conjugated with GalNAc, which interacts with ASGR thus mediating uptake of both ASOs (19,28,74). These GalNAc-ASOs were incubated with HepG2 cells where ASGR are expressed at relatively high levels, and STX5 and SEC31a were stained. Consistent with above observations, significant ASO–protein co-localization was detected for the PS-MOE ASO (Figure 9E), but not for the PO-MOE ASO (Figure 9F), although similar levels of cellular ASOs were observed. Together, these results further suggest that ASO–protein interactions play a role in directing STX5 re-localization to LEs upon ASO incubation.

DISCUSSION

ASO trafficking and proper release from endocytic pathways to reach the cellular RNA targets are essential steps to achieve antisense activity. Accumulating evidence has suggested that productive ASO release mainly occurs at LEs or MVBs (9,23,25,26,31,75). Though potential pathways of ASO release from membrane enclosed organelles have been proposed previously, such as membrane fusion mediated leakage (26), little is known regarding the detailed mechanisms and experimental evidence supporting the proposed models is sparse. Recently, we showed that ASO release from LEs might be mediated by a back-fusion process through ILVs (28,30), and interaction of proteins (e.g. ANXA2) with the limiting membranes of LEs may also facilitate ASO release (28). In the current study, we demonstrated that COPII vesicles can re-locate to LEs upon ASO incubation and may enhance ASO activity by facilitating ASO release from LEs.

In the absence of ASOs, COPII vesicles were barely detected to co-localize with LEs. However, upon ASO incubation, COPII/LE co-localization was readily observed, as determined by staining of different core coat proteins in different stable cell lines and primary cells. COPII re-localization to LEs is time-dependent, occurred ∼6–8 h after ASO incubation, and the co-localization event declined at later time (48 h), suggesting a dynamic process. These observations also indicate that COPII vesicles re-localize to LEs after ASOs accumulation in this organelle, as ASOs can local-

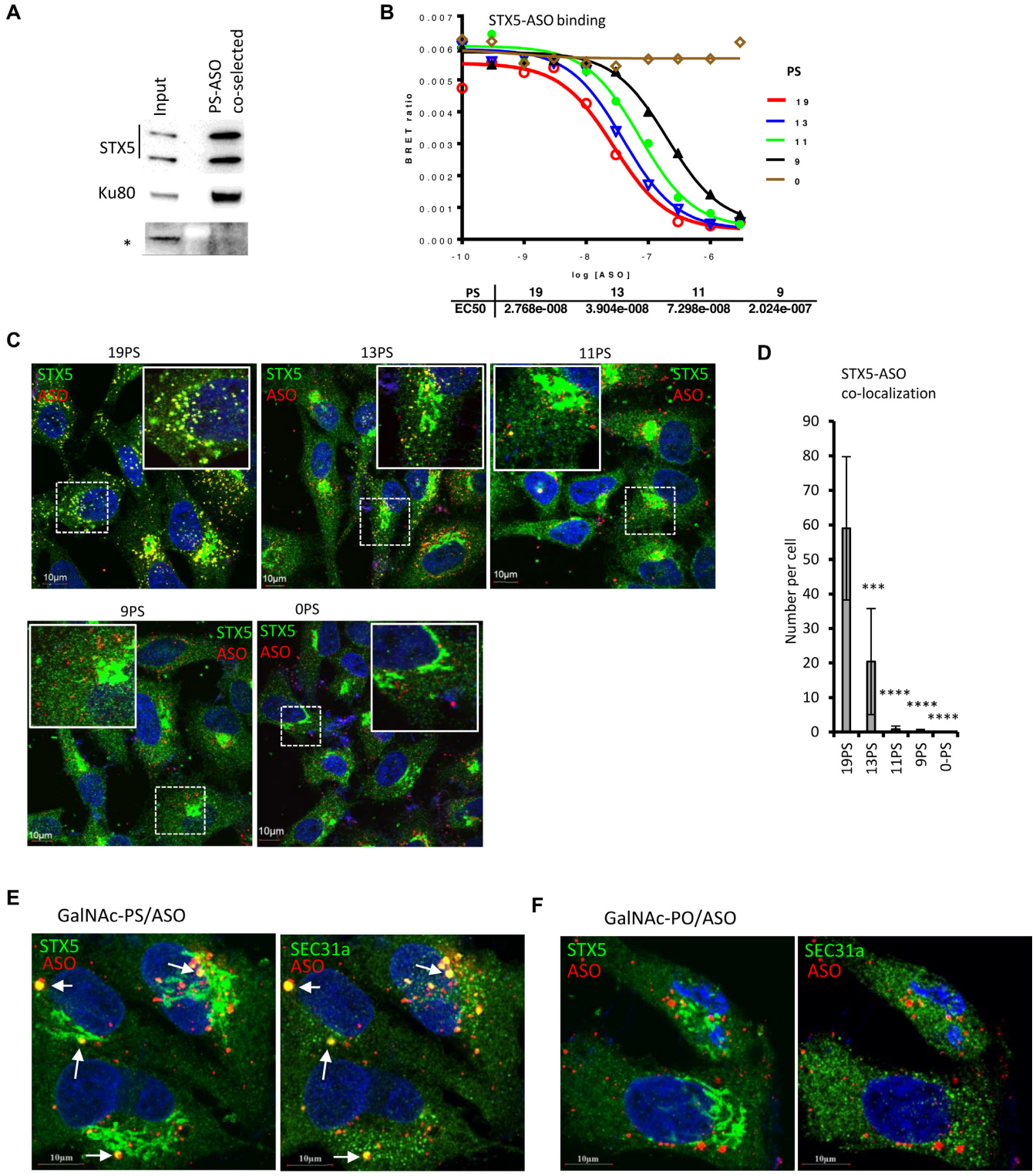

Figure 9. ASO/STX5 co-localization at LEs is most likely mediated by ASO–protein interactions. (**A**) Western analyses for STX5 protein co-selected with a biotinylated PS-MOE ASO. Ku80 was used as a positive control. *, a non-specific protein band. (**B**) BRET assay for binding of STX5 and ASOs (XL948-XL952) with different numbers of continuous PS using a competition study. The binding k_d are present below the curves. (**C**) Immunofluorescent staining of SEC31a and STX5 in HeLa cells incubated for 16 h with 3 μM Cy3-labeled ASOs (XL953-XL958) containing different numbers of PS-modified nucleotides, as indicated above the panels. ASO/Protein co-localization is exemplified with arrows. (**D**) Quantification of ASO/STX5 co-localization events. Error bars indicate standard deviations of co-localization events as determined from 20 cells. The experiments were performed twice and similar trends were observed. *P*-values were calculated based on unpaired *t*-test. ***, P<0.001; ****, P<0.0001. (**E**) Immunofluorescent staining of STX5 and SEC31a in HepG2 cells incubated with 2 μM GalNAc-conjugated ASO730437 linked with PS backbones. (**F**) Immunofluorescent staining of STX5 and SEC31a in HepG2 cells incubated with 2 μM GalNAc-conjugated ASO841226 linked with PO backbones; scale bars, 10 μm.

ize to LEs within 1–2 h (28). The co-localization time between ASO/COPII at LEs correlates with the time when ASOs exhibited antisense activity, implying a linkage between LE localization of COPII vesicles and ASO release from the membrane-enclosed endosomes.

The kinetics of ASO/COPII co-localization at LE appears to be slower than that of ASO-induced re-localization of ANXA2 to LEs, which appeared as early as 1 h and became more robust at 2–4 h after ASO incubation (28). As ANXA2 is present at EE and is required for transport from EE to LE (32), ANXA2 may co-translocate with ASOs from EE to LE, as evidenced by the re-localization of ANXA2 at ILVs, which could be formed during EE to LE maturation. The EE-LE transport can lead to an early onset of LE localization of ANXA2 after ASO incubation, although recruitment of ANXA2 from cytosol to the limiting membrane of LE may also occur later to further enhance ANXA2 re-localization to LE (28). However, COPII re-localization to LE was only weakly detected at 4–6 h, and became more robust at 8–10 h after ASO incubation, suggesting that COPII vesicles may join LE from cytosolic environment, and less likely by co-transport with ASOs from EE. This possibility is supported by the following observations: (i) no COPII localization at ILVs within LEs was observed; (ii) COPII vesicle was not detected to localize at EE with or without ASO incubation and (iii) partial overlap between COPII vesicles and LEs was often observed in the presence of ASOs, suggesting contacts between two membraned compartments.

On the other hand, ASO/COPII co-localization does not require *de novo* assembly of COPII vesicles at ERES, as reduction of either SEC12 or SEC16, ER proteins required for COPII assembly, did not abolish COPII re-localization at LE nor affect ASO activity at earlier time (72 h) after siRNA treatment. However, at later time after SEC16 reduction (96 h after siRNA treatment) both ASO activity and ASO/COPII co-localization were decreased, further implying a role of budded COPII in ASO activity. In addition, ASO-positive COPII vesicles did not co-localize with ERES and ERGIC, whereas ASO-negative COPII vesicles can normally localize to ERES and ERGIC, suggesting that ASO/COPII association may not occur during COPII assembly or during ER–Golgi transport to ERGIC. Thus, we favor the possibility that pre-assembled COPII vesicles from the ER–Golgi transport pathway re-locate to LEs upon ASO incubation. This possibility is also supported by the observations that treatment with chloroquine, a LE/Lysosome membrane disruption agent, quickly abolished COPII/ASO co-localization at LE, whereas treatment with the ER–Golgi transport inhibitor BFA did not. Although it is theoretically possible that COPII vesicles may assemble on LE membrane in the presence of ASOs, as neither SEC16 nor SEC12 was detected to re-locate to LE (data not shown), and reduction of either protein by siRNA treatment for 72 h did not abolish COPII/ASO co-localization at LE, this possibility seems less likely.

Since the five core proteins of COPII vesicles do not bind PS-ASOs, and transfected ASOs that are largely present outside endosomes/lysosomes also do not co-localize with COPII vesicles, COPII re-localization to LE is thus unlikely caused by direct interactions between ASO and COPII proteins. Interestingly, P115 and STX5 were found to be required for COPII/ASO co-localization at LEs. Reduction of these proteins impaired COPII/ASO co-localization at LEs and decreased ASO activity. As STX5 and P115 are known to be involved in tethering and fusion of COPII vesicles with Golgi membranes, it is possible that these proteins may interact with pre-assembled COPII vesicles to mediate COPII localization at LEs upon ASO incubation. This possibility is supported by the observations that (i) STX5 could re-locate to LEs after ASO incubation, with a similar kinetics as COPII/ASO co-localization; (ii) chloroquine treatment also abolished STX5 re-localization to LEs, similar to that of COPII vesicles and (iii) STX5 and COPII vesicles affect ASO activity most likely by acting on the same pathway (s), as no additive effect was observed when both STX5 and SEC31a were reduced.

Although STX5 reduction decreased ASO activity and inhibited ASO/COPII co-localization at LEs, reduction of SEC31a decreased ASO activity but did not abolish ASO/STX5 co-localization, suggesting that LE re-localization of STX5 alone was not sufficient to facilitate ASO release, and that the effects of STX5 on ASO activity were most likely mediated by COPII vesicles. STX5 exhibited significant binding affinity to PS-ASOs, as determined using BRET assays. Importantly, ASO/STX5 co-localization at LEs positively correlates with the binding property of STX5 with ASOs. PS-ASOs that bind STX5 with high affinity can induce the re-localization of STX5 (and COPII vesicles) to LEs, whereas ASOs with fewer PS backbone that bind STX5 with reduced affinity caused less LE re-localization of STX5, and the PO-ASO that does not bind STX5 failed to co-localize with STX5. It is thus likely that ASOs present in LEs may interact with STX5 protein, leading to re-localization of STX5 to LEs, which in turn recruits ER-budded COPII vesicles to LEs, in a way mediated by P115 (Figure 10A). In contrast, ANXA2 may co-transport with ASOs from EE to LEs and co-localize with ASOs at ILVs insides LEs, and may also be recruited from cytosol to the membrane of LEs, where they can facilitate ASO release, as proposed previously (28). Currently, it is unclear how and from where STX5 is recruited to LEs by ASOs present inside endosomes. It is possible that this event is mediated by other ASO-binding proteins that may traffic together with ASOs from EEs, or recruited from cytosol to LEs. Understanding the detailed mechanisms and identifying factors potentially mediating STX5 re-localization to LEs await further investigation.

The kinetics of COPII/ASO co-localization at LEs correlates with the time displaying antisense activity, suggesting that COPII/LE interaction may play a role in ensuring ASO activity. Indeed, reduction of COPII coat proteins, and not COPI proteins, in both HeLa and A431 cells significantly reduced ASO activity, further suggesting that COPII vesicles, and not the ER–Golgi transport pathway, facilitate ASO activity. Reduction of SEC31a did not impair ASO uptake and EE to LE transport, implying that COPII affects ASO activity at steps after ASO transport to LEs. On the other hand, reduction of SEC31a did not affect the activity of ASOs upon transfection, suggesting pathways or proteins required for ASO activity after release from membraned organelles were not affected. These observations suggest that ASO release from endosomes was impaired by reduction of

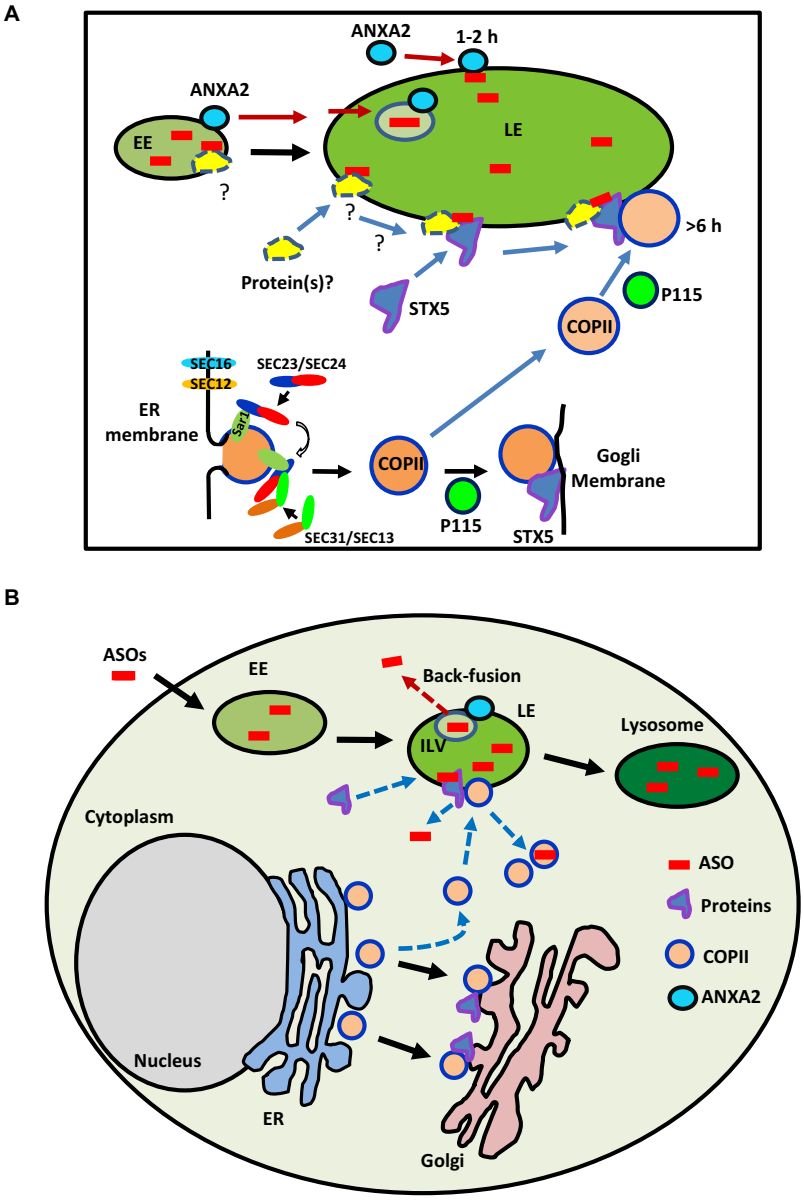

Figure 10. A proposed model for COPII vesicle-mediated ASO release from endosomes. (**A**) A potential pathway of COPII recruitment to the LEs upon ASO incubation. ASOs present in LEs can interact with STX5, leading to re-localization of STX5 to LEs. This process may be mediated by other ASO-binding proteins that can either translocate from EE to LE during ASO trafficking, or be recruited from cytosol upon ASO incubation, as indicated by question marks. LE-localized STX5 may in turn recruit COPII vesicles that are pre-assembled and budded from ER, in a way mediated by P115. STX5/COPII re-localization to LEs occurs at later time (6–8 h) after ASO incubation, in contrast to ANXA2, which can be co-transported from EE to LE during ASO trafficking, and re-locate to LEs within 1–2 h after ASO incubation, and can also be present in ILVs. (**B**) A proposed model for COPII-mediated ASO release from LEs. Upon internalization, ASOs enter EEs and LEs, and ultimately reach lysosomes. Accumulation of ASOs in LEs may recruit some proteins, including STX5 and other proteins, to LEs. These proteins can mediate the LE re-localization of COPII vesicles, which are pre-assembled at ERES and already leave ER. Interaction of COPII vesicles with LE may trigger membrane deformation, leading to ASO release from LE to the cytosol. On the other hand, COPII vesicles may also extract some ASOs from LEs. In addition, ASOs present in ILVs inside LEs can also be released via back-fusion processes mediated by ANXA2 and likely other proteins as well. Thus, in this model we show two independent pathways that can result in LE accumulation and release of PS-ASOs and we suspect that there are other pathways yet to be discovered.

COPII proteins. Indeed, kinetic studies after ASO removal from medium demonstrated that reduction of COPII proteins caused slower ASO release (Figure 5D).

Taken together, these results suggest a potential ASO release pathway that upon incubation, internalized ASOs via endocytic pathways can traffic through EE, transport to LEs and lysosomes (Figure 10B). ASO transport to LEs may re-locate certain proteins to LE membrane through ASO–protein interactions, and we have identified such an important protein, STX5, that binds to PS-ASOs. De-localized proteins, including STX5, may mediate re-localization of COPII vesicles to LE membrane. The interaction between the two membraned organelles can thus trigger ASO release from LEs to cytosol likely due to mem-

brane deformation, ensuring antisense activity. It is also possible that some ASOs may join COPII vesicles and leave LEs. Our results, combined with previous observations that ASOs can be released from ILVs via a back-fusion process (30), suggest that multiple pathways are involved in ASO release from endosomes. Further understanding ASO release pathways and detailed mechanisms will provide important information that can facilitate ASO drug design towards efficient and specific release from endosomes.

SUPPLEMENTARY DATA

Supplementary Data are available at NAR Online.

ACKNOWLEDGEMENTS

We wish to thank Dr Frank Bennett for stimulating discussions; Dr Tomas Kirchhausen for discussions and kindly providing GFP-Rab7 cell line; Joyee Yao for technique assistance.

FUNDING

Internal funding from Ionis Pharmaceuticals. Funding for open access charge: Ionis Pharmaceuticals internal funding.
Conflict of interest statement. None declared.

REFERENCES

1. Dias,N. and Stein,C.A. (2002) Antisense oligonucleotides: basic concepts and mechanisms. *Mol. Cancer Ther.*, **1**, 347–355.
2. Crooke,S.T., Vickers,T., Lima,W.F. and Wu,H.-J. (2008) Mechanisms of Antisense Drug Action, an Introduction. In: Crooke,ST (ed). *Antisense Drug Technology: Principles, Strategies, and Applications*. 2nd edn, CRC Press, Boca Raton, pp. 3–46.
3. Crooke,S.T., Witztum,J.L., Bennett,C.F. and Baker,B.F. (2018) RNA-Targeted therapeutics. *Cell metabolism*, **27**, 714–739.
4. Bennett,C.F., Baker,B.F., Pham,N., Swayze,E. and Geary,R.S. (2017) Pharmacology of antisense drugs. *Annu. Rev. Pharmacol. Toxicol.*, **57**, 81–105.
5. Bennett,C.F. and Swayze,E.E. (2010) RNA targeting therapeutics: molecular mechanisms of antisense oligonucleotides as a therapeutic platform. *Annu. Rev. Pharmacol. Toxicol.*, **50**, 259–293.
6. Swayze,E.E. and Bhat,B. (2008) The Medicinal Chemistry of Oligonucleotides. In: Crooke,ST (ed). *Antisense Drug Technology: Principles, Strategies, and Applications*. 2nd edn, CRC Press, Boca Raton, pp. 143–182.
7. Kurreck,J. (2003) Antisense technologies. Improvement through novel chemical modifications. *Eur. J. Biochem.*, **270**, 1628–1644.
8. Geary,R.S., Norris,D., Yu,R. and Bennett,C.F. (2015) Pharmacokinetics, biodistribution and cell uptake of antisense oligonucleotides. *Adv. Drug Deliv. Rev.*, **87**, 46–51.
9. Crooke,S.T., Wang,S., Vickers,T.A., Shen,W. and Liang,X.H. (2017) Cellular uptake and trafficking of antisense oligonucleotides. *Nat. Biotechnol.*, **35**, 230–237.
10. Brown,D.A., Kang,S.H., Gryaznov,S.M., DeDionisio,L., Heidenreich,O., Sullivan,S., Xu,X. and Nerenberg,M.I. (1994) Effect of phosphorothioate modification of oligodeoxynucleotides on specific protein binding. *J. Biol. Chem.*, **269**, 26801–26805.
11. Liang,X.H., Shen,W., Sun,H., Kinberger,G.A., Prakash,T.P., Nichols,J.G. and Crooke,S.T. (2016) Hsp90 protein interacts with phosphorothioate oligonucleotides containing hydrophobic 2′-modifications and enhances antisense activity. *Nucleic Acids Res.*, **44**, 3892–3907.
12. Shen,W., Liang,X.H., Sun,H. and Crooke,S.T. (2015) 2′-Fluoro-modified phosphorothioate oligonucleotide can cause rapid degradation of P54nrb and PSF. *Nucleic Acids Res.*, **43**, 4569–4578.
13. Liang,X.H., Sun,H., Shen,W. and Crooke,S.T. (2015) Identification and characterization of intracellular proteins that bind oligonucleotides with phosphorothioate linkages. *Nucleic Acids Res.*, **43**, 2927–2945.
14. Lima,W.F., Vickers,T.A., Nichols,J., Li,C. and Crooke,S.T. (2014) Defining the factors that contribute to on-target specificity of antisense oligonucleotides. *PLoS One*, **9**, e101752.
15. Vickers,T.A. and Crooke,S.T. (2015) The rates of the major steps in the molecular mechanism of RNase H1-dependent antisense oligonucleotide induced degradation of RNA. *Nucleic Acids Res.*, **43**, 8955–8963.
16. Liang,X.H., Nichols,J.G., Sun,H. and Crooke,S.T. (2018) Translation can affect the antisense activity of RNase H1-dependent oligonucleotides targeting mRNAs. *Nucleic Acids Res.*, **46**, 293–313.
17. Geary,R.S. (2009) Antisense oligonucleotide pharmacokinetics and metabolism. *Expert Opin. Drug Metab. Toxicol.*, **5**, 381–391.
18. Juliano,R.L., Ming,X. and Nakagawa,O. (2012) Cellular uptake and intracellular trafficking of antisense and siRNA oligonucleotides. *Bioconjug. Chem.*, **23**, 147–157.
19. Tanowitz,M., Hettrick,L., Revenko,A., Kinberger,G.A., Prakash,T.P. and Seth,P.P. (2017) Asialoglycoprotein receptor 1 mediates productive uptake of N-acetylgalactosamine-conjugated and unconjugated phosphorothioate antisense oligonucleotides into liver hepatocytes. *Nucleic Acids Res.*, **45**, 12388–12400.
20. Miller,C.M., Donner,A.J., Blank,E.E., Egger,A.W., Kellar,B.M., Ostergaard,M.E., Seth,P.P. and Harris,E.N. (2016) Stabilin-1 and Stabilin-2 are specific receptors for the cellular internalization of phosphorothioate-modified antisense oligonucleotides (ASOs) in the liver. *Nucleic Acids Res.*, **44**, 2782–2794.
21. Wang,S., Allen,N., Vickers,T.A., Revenko,A.S., Sun,H., Liang,X.H. and Crooke,S.T. (2018) Cellular uptake mediated by epidermal growth factor receptor facilitates the intracellular activity of phosphorothioate-modified antisense oligonucleotides. *Nucleic Acids Res.*, **46**, 3579–3594.
22. Beltinger,C., Saragovi,H.U., Smith,R.M., LeSauteur,L., Shah,N., DeDionisio,L., Christensen,L., Raible,A., Jarett,L. and Gewirtz,A.M. (1995) Binding, uptake and intracellular trafficking of phosphorothioate-modified oligodeoxynucleotides. *J. Clin. Invest.*, **95**, 1814–1823.
23. Juliano,R.L., Carver,K., Cao,C. and Ming,X. (2013) Receptors, endocytosis, and trafficking: the biological basis of targeted delivery of antisense and siRNA oligonucleotides. *J. Drug Target.*, **21**, 27–43.
24. Juliano,R.L. and Carver,K. (2015) Cellular uptake and intracellular trafficking of oligonucleotides. *Adv. Drug. Deliv. Rev.*, **87**, 35–45.
25. Koller,E., Vincent,T.M., Chappell,A., De,S., Manoharan,M. and Bennett,C.F. (2011) Mechanisms of single-stranded phosphorothioate modified antisense oligonucleotide accumulation in hepatocytes. *Nucleic Acids Res.*, **39**, 4795–4807.
26. Juliano,R.L. (2016) The delivery of therapeutic oligonucleotides. *Nucleic Acids Res.*, **44**, 6518–6548.
27. Dowdy,S.F. (2017) Overcoming cellular barriers for RNA therapeutics. *Nat. Biotechnol.*, **35**, 222–229.
28. Wang,S., Sun,H., Tanowitz,M., Liang,X.H. and Crooke,S.T. (2016) Annexin A2 facilitates endocytic trafficking of antisense oligonucleotides. *Nucleic Acids Res.*, **44**, 7314–7330.
29. Yang,B., Ming,X., Cao,C., Laing,B., Yuan,A., Porter,M.A., Hull-Ryde,E.A., Maddry,J., Suto,M., Janzen,W.P. *et al.* (2015) High-throughput screening identifies small molecules that enhance the pharmacological effects of oligonucleotides. *Nucleic Acids Res.*, **43**, 1987–1996.
30. Wang,S., Sun,H., Tanowitz,M., Liang,X.H. and Crooke,S.T. (2017) Intra-endosomal trafficking mediated by lysobisphosphatidic acid contributes to intracellular release of phosphorothioate-modified antisense oligonucleotides. *Nucleic Acids Res.*, **45**, 5309–5322.
31. Juliano,R.L., Wang,L., Tavares,F., Brown,E.G., James,L., Ariyarathna,Y., Ming,X., Mao,C. and Suto,M. (2018) Structure-activity relationships and cellular mechanism of action of small molecules that enhance the delivery of oligonucleotides. *Nucleic Acids Res.*, **46**, 1601–1613.
32. Morel,E. and Gruenberg,J. (2009) Annexin A2 binding to endosomes and functions in endosomal transport are regulated by tyrosine 23 phosphorylation. *J. Biol. Chem.*, **284**, 1604–1611.
33. Kobayashi,T., Stang,E., Fang,K.S., de Moerloose,P., Parton,R.G. and Gruenberg,J. (1998) A lipid associated with the antiphospholipid

syndrome regulates endosome structure and function. *Nature*, **392**, 193–197.
34. Barlowe,C., Orci,L., Yeung,T., Hosobuchi,M., Hamamoto,S., Salama,N., Rexach,M.F., Ravazzola,M., Amherdt,M. and Schekman,R. (1994) COPII: a membrane coat formed by Sec proteins that drive vesicle budding from the endoplasmic reticulum. *Cell*, **77**, 895–907.
35. Zanetti,G., Pahuja,K.B., Studer,S., Shim,S. and Schekman,R. (2011) COPII and the regulation of protein sorting in mammals. *Nat. Cell Biol.*, **14**, 20–28.
36. D'Arcangelo,J.G., Stahmer,K.R. and Miller,E.A. (2013) Vesicle-mediated export from the ER: COPII coat function and regulation. *Biochim. Biophys. Acta*, **1833**, 2464–2472.
37. Budnik,A. and Stephens,D.J. (2009) ER exit sites–localization and control of COPII vesicle formation. *FEBS Lett.*, **583**, 3796–3803.
38. Bethune,J. and Wieland,F.T. (2018) Assembly of COPI and COPII vesicular coat proteins on membranes. *Annu. Rev. Biophys.*, **47**, 63–83.
39. Miller,E.A. and Barlowe,C. (2010) Regulation of coat assembly–sorting things out at the ER. *Curr. Opin. Cell Biol.*, **22**, 447–453.
40. Barlowe,C. and Schekman,R. (1993) SEC12 encodes a guanine-nucleotide-exchange factor essential for transport vesicle budding from the ER. *Nature*, **365**, 347–349.
41. Montegna,E.A., Bhave,M., Liu,Y., Bhattacharyya,D. and Glick,B.S. (2012) Sec12 binds to Sec16 at transitional ER sites. *PLoS One*, **7**, e31156.
42. Watson,P., Townley,A.K., Koka,P., Palmer,K.J. and Stephens,D.J. (2006) Sec16 defines endoplasmic reticulum exit sites and is required for secretory cargo export in mammalian cells. *Traffic*, **7**, 1678–1687.
43. Hughes,H. and Stephens,D.J. (2008) Assembly, organization, and function of the COPII coat. *Histochem. Cell Biol.*, **129**, 129–151.
44. Haucke,V. (2003) Vesicle budding: a coat for the COPs. *Trends Cell Biol.*, **13**, 59–60.
45. Lord,C., Ferro-Novick,S. and Miller,E.A. (2013) The highly conserved COPII coat complex sorts cargo from the endoplasmic reticulum and targets it to the golgi. *Cold Spring Harb. Perspect. Biol.*, **5**, 1–13.
46. Brandizzi,F. and Barlowe,C. (2013) Organization of the ER-Golgi interface for membrane traffic control. *Nat. rev. Mol. Cell Biol.*, **14**, 382–392.
47. Barlowe,C. (1997) Coupled ER to Golgi transport reconstituted with purified cytosolic proteins. *J. Cell Biol.*, **139**, 1097–1108.
48. Cao,X., Ballew,N. and Barlowe,C. (1998) Initial docking of ER-derived vesicles requires Uso1p and Ypt1p but is independent of SNARE proteins. *EMBO J.*, **17**, 2156–2165.
49. Wang,T., Grabski,R., Sztul,E. and Hay,J.C. (2015) p115-SNARE interactions: a dynamic cycle of p115 binding monomeric SNARE motifs and releasing assembled bundles. *Traffic*, **16**, 148–171.
50. Allan,B.B., Moyer,B.D. and Balch,W.E. (2000) Rab1 recruitment of p115 into a cis-SNARE complex: programming budding COPII vesicles for fusion. *Science*, **289**, 444–448.
51. Rowe,T., Dascher,C., Bannykh,S., Plutner,H. and Balch,W.E. (1998) Role of vesicle-associated syntaxin 5 in the assembly of pre-Golgi intermediates. *Science*, **279**, 696–700.
52. Liang,X.H., Shen,W., Sun,H., Prakash,T.P. and Crooke,S.T. (2014) TCP1 complex proteins interact with phosphorothioate oligonucleotides and can co-localize in oligonucleotide-induced nuclear bodies in mammalian cells. *Nucleic Acids Res.*, **42**, 7819–7832.
53. Vickers,T.A. and Crooke,S.T. (2016) Development of a quantitative BRET affinity assay for nucleic Acid-Protein interactions. *PLoS One*, **11**, e0161930.
54. Tillmann,K.D., Reiterer,V., Baschieri,F., Hoffmann,J., Millarte,V., Hauser,M.A., Mazza,A., Atias,N., Legler,D.F., Sharan,R. *et al.* (2015) Regulation of Sec16 levels and dynamics links proliferation and secretion. *J. Cell Sci.*, **128**, 670–682.
55. Liang,X.H., Vickers,T.A., Guo,S. and Crooke,S.T. (2011) Efficient and specific knockdown of small non-coding RNAs in mammalian cells and in mice. *Nucleic Acids Res.*, **39**, e13.
56. Liang,X.H., Sun,H., Nichols,J.G. and Crooke,S.T. (2017) RNase H1-dependent antisense oligonucleotides are robustly active in directing RNA cleavage in both the cytoplasm and the nucleus. *Mol. Ther.*, **25**, 2075–2092.
57. Humphries,W.H.T., Szymanski,C.J. and Payne,C.K. (2011) Endo-lysosomal vesicles positive for Rab7 and LAMP1 are terminal vesicles for the transport of dextran. *PLoS One*, **6**, e26626.
58. Mayle,K.M., Le,A.M. and Kamei,D.T. (2012) The intracellular trafficking pathway of transferrin. *Biochim. Biophys. Acta*, **1820**, 264–281.
59. Wang,J., Davis,S., Zhu,M., Miller,E.A. and Ferro-Novick,S. (2017) Autophagosome formation: where the secretory and autophagy pathways meet. *Autophagy*, **13**, 973–974.
60. Shen,W., Liang,X.H. and Crooke,S.T. (2014) Phosphorothioate oligonucleotides can displace NEAT1 RNA and form nuclear paraspeckle-like structures. *Nucleic Acids Res.*, **42**, 8648–8662.
61. Bennett,C.F., Chiang,M.Y., Chan,H., Shoemaker,J.E. and Mirabelli,C.K. (1992) Cationic lipids enhance cellular uptake and activity of phosphorothioate antisense oligonucleotides. *Mol. Pharmacol.*, **41**, 1023–1033.
62. Szul,T. and Sztul,E. (2011) COPII and COPI traffic at the ER-Golgi interface. *Physiology (Bethesda)*, **26**, 348–364.
63. Jensen,D. and Schekman,R. (2011) COPII-mediated vesicle formation at a glance. *J. Cell Sci.*, **124**, 1–4.
64. Sprangers,J. and Rabouille,C. (2015) SEC16 in COPII coat dynamics at ER exit sites. *Biochem. Soc. Trans.*, **43**, 97–103.
65. Jiang,S., Rhee,S.W., Gleeson,P.A. and Storrie,B. (2006) Capacity of the Golgi apparatus for cargo transport prior to complete assembly. *Mol. Biol. Cell*, **17**, 4105–4117.
66. Laufman,O., Hong,W. and Lev,S. (2013) The COG complex interacts with multiple Golgi SNAREs and enhances fusogenic assembly of SNARE complexes. *J. Cell Sci.*, **126**, 1506–1516.
67. Grabski,R., Balklava,Z., Wyrozumska,P., Szul,T., Brandon,E., Alvarez,C., Holloway,Z.G. and Sztul,E. (2012) Identification of a functional domain within the p115 tethering factor that is required for Golgi ribbon assembly and membrane trafficking. *J. Cell Sci.*, **125**, 1896–1909.
68. Geng,L., Boehmerle,W., Maeda,Y., Okuhara,D.Y., Tian,X., Yu,Z., Choe,C.U., Anyatonwu,G.I., Ehrlich,B.E. and Somlo,S. (2008) Syntaxin 5 regulates the endoplasmic reticulum channel-release properties of polycystin-2. *Proc. Natl. Acad. Sci. U.S.A.*, **105**, 15920–15925.
69. Nonnenmacher,M.E., Cintrat,J.C., Gillet,D. and Weber,T. (2015) Syntaxin 5-dependent retrograde transport to the trans-Golgi network is required for adeno-associated virus transduction. *J. Virol.*, **89**, 1673–1687.
70. Shitara,A., Shibui,T., Okayama,M., Arakawa,T., Mizoguchi,I., Sakakura,Y. and Takuma,T. (2013) VAMP4 is required to maintain the ribbon structure of the Golgi apparatus. *Mol. Cell Biochem.*, **380**, 11–21.
71. Progida,C. and Bakke,O. (2016) Bidirectional traffic between the Golgi and the endosomes - machineries and regulation. *J. Cell Sci.*, **129**, 3971–3982.
72. Hong,W. (2005) SNAREs and traffic. *Biochim. Biophys. Acta*, **1744**, 120–144.
73. Sohda,M., Misumi,Y., Yoshimura,S., Nakamura,N., Fusano,T., Sakisaka,S., Ogata,S., Fujimoto,J., Kiyokawa,N. and Ikehara,Y. (2005) Depletion of vesicle-tethering factor p115 causes mini-stacked Golgi fragments with delayed protein transport. *Biochem. Biophys. Res. Commun.*, **338**, 1268–1274.
74. Prakash,T.P., Graham,M.J., Yu,J., Carty,R., Low,A., Chappell,A., Schmidt,K., Zhao,C., Aghajan,M., Murray,H.F. *et al.* (2014) Targeted delivery of antisense oligonucleotides to hepatocytes using triantennary N-acetyl galactosamine improves potency 10-fold in mice. *Nucleic Acids Res.*, **42**, 8796–8807.
75. Juliano,R.L., Ming,X., Carver,K. and Laing,B. (2014) Cellular uptake and intracellular trafficking of oligonucleotides: implications for oligonucleotide pharmacology. *Nucleic Acid Ther.*, **24**, 101–113.